U.S. Department of the Interior
U.S. Geological Survey

Geology, Age, and Tectonic Setting of the Cretaceous Sliderock Mountain Volcano, Montana

U.S. Geological Survey Professional Paper 1602

Availability of Publications of the U.S. Geological Survey

Order U.S. Geological Survey (USGS) publications from the offices listed below. Detailed ordering instructions, along with prices of the last offerings, are given in the current-year issues of the catalog "New Publications of the U.S. Geological Survey."

Books, Maps, and Other Publications

By Mail

Books, maps, and other publications are available by mail from—

USGS Information Services
Box 25286, Federal Center
Denver, CO 80225

Publications include Professional Papers, Bulletins, Water-Supply Papers, Techniques of Water-Resources Investigations, Circulars, Fact Sheets, publications of general interest, single copies of permanent USGS catalogs, and topographic and thematic maps.

Over the Counter

Books, maps, and other publications of the U.S. Geological Survey are available over the counter at the following USGS Earth Science Information Centers (ESIC's), all of which are authorized agents of the Superintendent of Documents:

- Anchorage, Alaska–Rm. 101, 4230 University Dr.
- Denver, Colorado–Bldg. 810, Federal Center
- Menlo Park, California–Rm. 3128, Bldg. 3, 345 Middlefield Rd.
- Reston, Virginia–Rm. 1C402, USGS National Center, 12201 Sunrise Valley Dr.
- Salt Lake City, Utah–2222 West, 2300 South (books and maps available for inspection only)
- Spokane, Washington–Rm. 135, U.S. Post Office Building, 904 West Riverside Ave.
- Washington, D.C.–Rm. 2650, Main Interior Bldg., 18th and C Sts., NW.

Maps only may be purchased over the counter at the following USGS office:

- Rolla, Missouri–1400 Independence Rd.

Electronically

Some USGS publications, including the catalog "New Publications of the U.S. Geological Survey" are also available electronically on the USGS's World Wide Web home page at **http://www.usgs.gov**

Preliminary Determination of Epicenters

Subscriptions to the periodical "Preliminary Determination of Epicenters" can be obtained only from the Superintendent of Documents. Check or money order must be payable to the Superintendent of Documents. Order by mail from—

Superintendent of Documents
Government Printing Office
Washington, DC 20402

Information Periodicals

Many Information Periodicals products are available through the systems or formats listed below:

Printed Products

Printed copies of the Minerals Yearbook and the Mineral Commodity Summaries can be ordered from the Superintendent of Documents, Government Printing Office (address above). Printed copies of Metal Industry Indicators and Mineral Industry Surveys can be ordered from the Center for Disease Control and Prevention, National Institute for Occupational Safety and Health, Pittsburgh Research Center, P.O. Box 18070, Pittsburgh, PA 15236–0070.

Mines FaxBack: Return fax service

1. Use the touch-tone handset attached to your fax machine's telephone jack. (ISDN [digital] telephones cannot be used with fax machines.)
2. Dial (703) 648–4999.
3. Listen to the menu options and punch in the number of your selection, using the touch-tone telephone.
4. After completing your selection, press the start button on your fax machine.

CD-ROM

A disc containing chapters of the Minerals Yearbook (1993–95), the Mineral Commodity Summaries (1995–97), a statistical compendium (1970–90), and other publications is updated three times a year and sold by the Superintendent of Documents, Government Printing Office (address above).

World Wide Web

Minerals information is available electronically at **http://minerals.er.usgs.gov/minerals/**

Subscription to the catalog "New Publications of the U.S. Geological Survey"

Those wishing to be placed on a free subscription list for the catalog "New Publications of the U.S. Geological Survey" should write to—

U.S. Geological Survey
903 National Center
Reston, VA 20192

Geology, Age, and Tectonic Setting of the Cretaceous Sliderock Mountain Volcano, Montana

By Edward A. du Bray *and* Stephen S. Harlan

U.S. GEOLOGICAL SURVEY PROFESSIONAL PAPER 1602

Physical and compositional development of an Upper Cretaceous stratovolcano in south-central Montana

UNITED STATES GOVERNMENT PRINTING OFFICE, WASHINGTON : 1998

U.S. DEPARTMENT OF THE INTERIOR
BRUCE BABBITT, Secretary

U.S. GEOLOGICAL SURVEY
Thomas J. Casadevall, Acting Director

For sale by U.S. Geological Survey, Information Services
Box 25286, Federal Center
Denver, CO 80225

Library of Congress Cataloging-in-Publication Data

Du Bray, E.A.
Geology and tectonic setting of the Cretaceous Sliderock Mountain volcano, Montana / by Edward A. du Bray and Stephen S. Harlan.
p. cm. — (U.S. Geological Survey professional paper ; 1602)
Includes bibliographical references.
1. Sliderock Mountain (Sweet Grass County, Mont.). 2. Geology, Stratigraphic—Cretaceous. 3. Geology—Montana—Sliderock Mountain (Sweet Grass County). 4. Volcanoes—Montana—Sweet Grass County. I. Harlan, Stephen S. II. Title. III. Series.
QE523.S63D8 1999
551.2'1'0978664—dc21 98–18106
CIP

CONTENTS

FIGURES

TABLES

Geology, Age, and Tectonic Setting of the Cretaceous Sliderock Mountain Volcano, Montana

By Edward A. du Bray *and* Stephen S. Harlan

ABSTRACT

Sliderock Mountain volcano is an Upper Cretaceous stratovolcano located along the southern margin of the Crazy Mountains Basin in south-central Montana. The volcano is part of an extensive northwest-trending volcanic field that lies astride the folds and faults of the Nye-Bowler lineament. The volcano consists mostly of volcaniclastic strata, although basaltic andesite lava flows are also present. An extensively eroded, weakly mineralized hypabyssal intrusive complex, inferred to represent the volcano's solidified magma chamber, intrudes lava flows and associated lahars. $^{40}Ar/^{39}Ar$ data indicate that the oldest lavas associated with the volcano were erupted by about 78±1 Ma, whereas dikes representing the final phase of magmatism were emplaced about 74.9 Ma.

The magmatic system ranges in composition from basaltic andesite to dacite. Major oxide and trace element data are consistent with a subduction-related continental magmatic arc setting. However, this type of magmatic activity was not widespread in this region during Late Cretaceous time. The Sliderock Mountain volcano represents one of the easternmost manifestations of Late Cretaceous magmatic activity and, except for rocks of the Boulder batholith and cogenetic Elkhorn Mountains Volcanics 160 km to the northwest, is rare in south-central Montana. Compositional diversity within components of the volcano appears to reflect evolution via about 50 percent fractional crystallization involving clinopyroxene and plagioclase. During the compositional evolution of the magma system, the reservoir was periodically tapped to feed lava flows, dikes, and a series of coalesced hypabyssal stocks. The location of Sliderock Mountain volcano, as well as other igneous rocks of this field, may have been controlled to some extent by the deep-seated fault system of the Nye-Bowler lineament.

INTRODUCTION AND GEOLOGIC SETTING

An extensive field of Upper Cretaceous volcanic rocks is exposed along the southern margin of the Crazy Mountains Basin, north of the Beartooth Mountains, in south-central Montana. These volcanic rocks have long been considered part of the Upper Cretaceous Livingston Group, exposed elsewhere in the Crazy Mountains, but clearly represent a proximal, physically distinct volcanic source area. These rocks are important in understanding the geologic and tectonic setting of the northern Rocky Mountains because they constitute one of the easternmost Late Cretaceous volcanic fields in the North American Cordillera. The volcanic, volcaniclastic, and intrusive rocks that comprise this field have been described by a number of workers including Weed (1893), Vhay (1934), Rouse and others (1937), Parsons (1942), and Brozdowski (1983), but in general, modern petrologic, geochemical, and geochronologic data are lacking for these rocks. In this report, we present new geologic, petrologic, geochemical, and $^{40}Ar/^{39}Ar$ geochronologic data from the informally named Sliderock Mountain volcano, one of the main volcanic centers in this field. The rocks that comprise the Sliderock Mountain volcano were studied as part of the U.S. Geological Survey's mapping efforts in U.S. Forest Service lands of the Custer-Gallatin National Forest (du Bray and others, 1994). The data obtained in this study are used to present a model for the genesis of the Sliderock Mountain volcano and to help define the regional tectono-magmatic regime in which it developed. The data and interpretations presented here, although largely limited to one volcanic center, provide a foundation for future, more detailed studies of the volcanic rocks that constitute this important Late Cretaceous volcanic field.

Sliderock Mountain volcano is located along the southern margin of the Crazy Mountains Basin (fig. 1), a complex, structural and physiographic basin in south-central Montana. The Crazy Mountains Basin originally developed as part of the Cordilleran foredeep that formed east of the Cordilleran orogenic belt during Mesozoic contraction associated with subduction of the Farallon plate along the western margin of North America (Dickinson and others, 1988). During the Late Cretaceous, the Crazy Mountains Basin received about 3500 m of volcaniclastic and synorogenic sediments derived primarily from volcanic and tectonic activity within the adjacent thrust belt to the west, as well as locally derived volcanic, volcaniclastic, and sedimentary rocks from vents located along the present-day southern margin of the basin. The original configuration of the Crazy Mountains Basin was

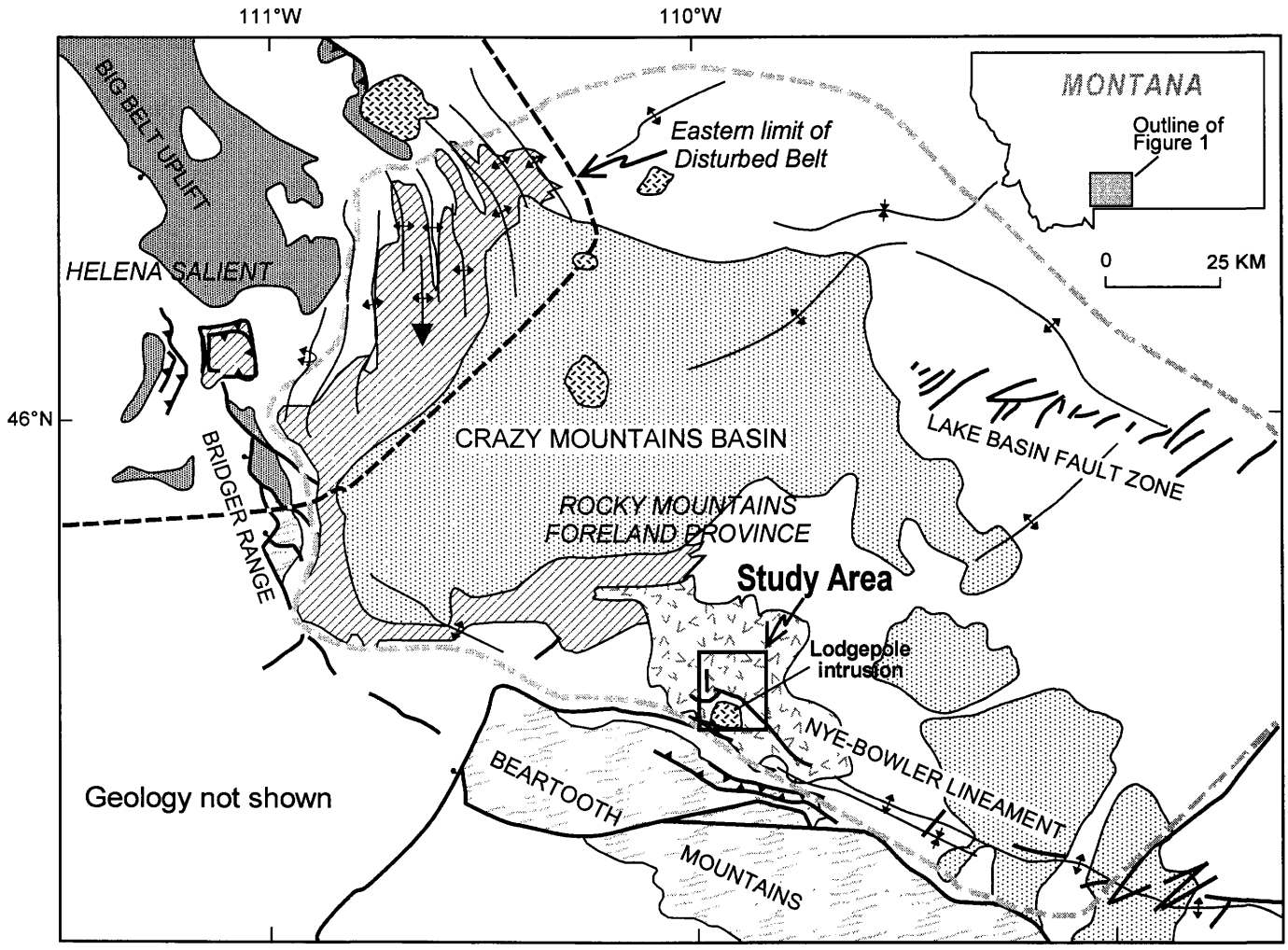

EXPLANATION

- Tertiary Fort Union Formation
- Tertiary/Cretaceous intrusive rocks
- Cretaceous rocks of the Sliderock Mountain volcano
- Cretaceous volcaniclastic rocks (Livingston Group)
- Phanerozoic sedimentary rocks
- Proterozoic Belt Supergroup
- Archean crystalline basement rocks
- Fault--Sense of displacement unspecified
- Normal fault--Ball and bar on downthrown block
- Thrust fault--Barb on upper plate
- Anticline--Arrow at end of line shows direction of fold plunge
- Overturned anticline
- Syncline

Figure 1. Map of the Crazy Mountains Basin in south-central Montana showing principal structural and tectonic features (modified from Roberts, 1972 and Harlan and others, 1988). Gray dashed line shows the approximate margins of the Crazy Mountains Basin.

substantially modified by the progression of thrust-belt folds and faults of the Helena Salient of the Disturbed Belt into the western part of the Crazy Mountains Basin during Late Cretaceous/early Tertiary time, followed by or coeval with development of basement-cored foreland uplifts of the Bridger Range and Beartooth uplifts, and by left-lateral movement along the Lake Basin and Nye-Bowler fault systems (Wilson, 1936; Roberts, 1972; Dickinson and others, 1988; Harlan and others, 1988).

The rocks of the Sliderock Mountain volcano are part of a northwest-trending belt of Upper Cretaceous volcanic and volcaniclastic rocks and their vents, which lie astride the northwest-trending axis of the Nye-Bowler lineament just north of the Beartooth uplift. These volcanic rocks have been considered part of the Livingston Group, a thick succession of dominantly fine grained volcaniclastic sandstone exposed primarily in the western part of the Crazy Mountains Basin (fig. 1). Although correlated with the Livingston Group, the exact relationship between the volcanic rocks exposed along the southern margin of the basin and those of the Livingston Group rocks is uncertain (Roberts, 1972). In general, Livingston Group sedimentary rocks are distal sediments derived from volcanic rocks associated with the Upper Cretaceous Elkhorn Mountains Volcanics exposed far to the northwest. The volcanic and very coarse grained volcaniclastic rocks exposed along the southern margin of the basin contrast significantly with the generally fine grained nature of the Livingston Group sedimentary rocks at their type section near Livingston, Mont. The presence of numerous vents, small stocks, dikes, and lava flows as well as the coarse-grained nature of the volcaniclastic rocks suggest that these represent a separate volcanic source area local to the southern Crazy Mountains Basin. Proximal volcaniclastic sedimentary rocks from these vents were shed northward and eastward and intermingled with more distal volcanic Livingston Group deposits derived from the Elkhorn Mountains volcanic centers far to the north and west.

Sliderock Mountain volcano (fig. 2) is an intermediate composition stratovolcano that consists primarily of volcaniclastic strata including lahars, mudflow deposits, volcaniclastic sandstone, and volumetrically minor pyroclastic flows. Intercalated with the volcaniclastic strata are basaltic andesite lava flows. The lava flows and volcaniclastic strata are cut by an intermediate composition hypabyssal stock, the diorite to granodiorite of Sliderock Mountain, which is inferred to be the solidified core of the volcano. Other minor stocks and plugs in the study area, including the Lodgepole intrusion (Brozdowski, 1983), which is well exposed in Clover Basin (fig. 2), are probably related to this intrusion. The stock and volcanic and volcaniclastic strata are cut by a swarm of dikes that form a crudely radial pattern along the north, east, and west flanks of the volcano. The dikes, whose orientation probably indicates a radially oriented stress regime related to shallow emplacement of the magma reservoir parental to the Sliderock Mountain volcano, was the final episode of magmatism associated with the volcano.

The volcano developed within a terrane underlain by Paleozoic and Mesozoic sedimentary rocks, the oldest of which are Paleozoic strata that form isolated roof pendants, large xenoliths, or are host rocks to the intrusive core of the volcano. Lower and Upper Cretaceous rocks, including the Kootenai Formation, Thermopolis and Mowry Shales, Frontier Formation, Cody Shale, Telegraph Creek Formation, and Eagle Sandstone, are intruded by the diorite to granodiorite of Sliderock Mountain and related intrusions. The intrusions have locally metamorphosed host sedimentary strata to an assemblage of calc-silicate minerals, including garnet and epidote. Where these rocks are most intensely metamorphosed, small bodies of weakly mineralized magnetite-garnet-epidote skarn are present. These skarns contain some sulfide minerals, especially chalcopyrite, and anomalous abundances of metals such as Au, Mo, Pb, Ag, Cu, and Sb (Hammarstrom and others, 1993). Numerous gold-bearing quartz veins are present in the area around Gold Hill (Crow, Gold Hill, Silver King, and Sulphide mines) (fig. 2). The diorite to granodiorite of Sliderock Mountain is locally weakly sericitized and contains disseminated pyrite near the veins. Gold placer deposits of limited size are present in the drainages near the gold-bearing veins.

PHYSICAL VOLCANOLOGY OF THE SLIDEROCK MOUNTAIN VOLCANO

The earliest volcanic activity associated with the stratovolcano was the eruption of basaltic andesite lava flows of Derby Ridge (du Bray and others, 1994). These rocks form a 400-m-thick section of lava flows, with volumetrically minor pyroclastic flows, block and ash flows, welded tuff, and interbedded lahars, erupted and unconformably deposited on moderately tilted Mesozoic sedimentary rocks.

The basaltic andesite lava flows are overlain by texturally and compositionally immature volcaniclastic strata. The basal approximately 50 m of these strata consist of interbedded sandstone, siltstone, and shale that probably forms the base of the Livingston Group in the area. These sedimentary rocks are overlain by at least 300 m of clast-supported lahar deposits (fig. 3) composed of poorly sorted, bouldery mudflows correlative with the Livingston Group (Parsons, 1942; p. 1177). The lahars, which form prominent rubbly cliffs, were probably derived by disaggregation of lavas erupted from the Sliderock Mountain volcano. Individual mudflows are massive and tens of meters thick; bedding is absent or poorly developed in most places. Clasts, dominantly composed of basaltic andesite, are 0.05–3 m in diameter and subangular to angular; some clasts in the basal part of the unit may be derived from the Lodgepole intrusion of Brozdowski (1983). The matrix of the deposits is finely

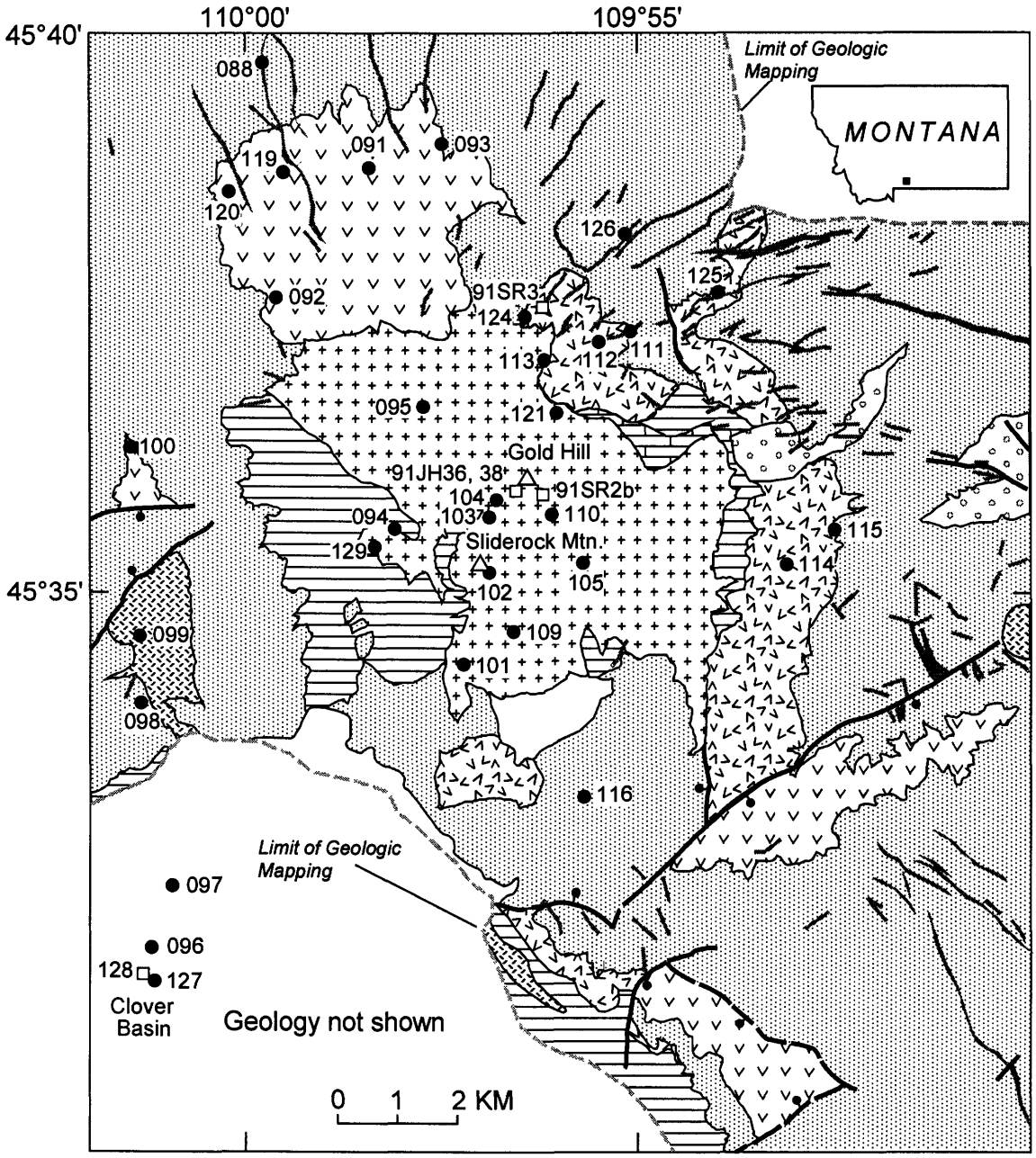

Figure 2 (above and facing page). Simplified geologic map showing the Sliderock Mountain stratovolcano (modified from du Bray and others, 1994). All three-digit sample locality numbers are prefixed by 202.

comminuted ash and altered andesite. This unit contains thin interbeds of very well sorted epiclastic volcanic sandstone, siltstone, and shale that contain carbonized plant remains; minor pyroclastic flow deposits may also be present. A few thin (several meters) andesite lava flows are enclosed within the lahar sequence. A second, 300-m-thick set of porphyritic, light- to dark-gray plagioclase-clinopyroxene basaltic andesite lava flows overlie the lahar deposits; these rocks probably represent the culmination of eruptive activity at the Sliderock Mountain center.

The intrusive phase of the Sliderock Mountain volcano is a very light gray to medium-gray plagioclase-hornblende diorite to granodiorite that intrudes all lava flow and lahar deposits. The diorite to granodiorite may represent multiple intrusive phases that coalesced to form an intrusive complex. The intrusive complex probably is the solidified core of the stratovolcano.

Porphyritic, light-gray plagioclase-clinopyroxene-hornblende basaltic trachyandesite to trachyte dikes, 1.5 to 5 km long and 1 to 10 m wide, form prominent, linear ridges,

EXPLANATION

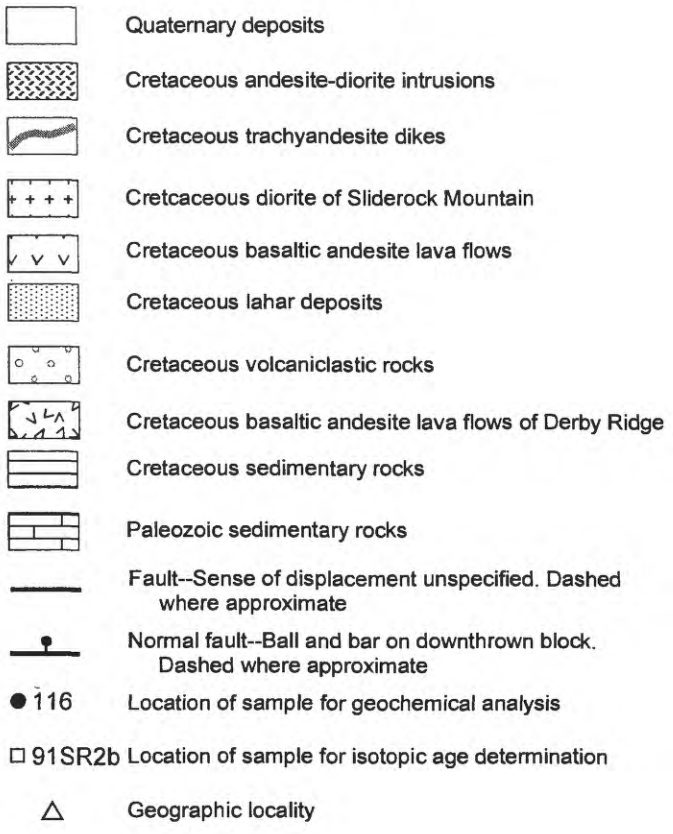

especially north of Sliderock Mountain. The dikes form a crudely radial pattern and cut all intrusive and extrusive phases of the volcano (du Bray and others, 1994). The dikes are compositionally and petrographically similar to other igneous rocks of the Sliderock Mountain area. They probably represent the final phase of igneous activity associated with the volcano. Other intrusive rocks, possibly contemporaneous with and genetically related to the dikes, include sills of light-gray porphyritic andesite, a plug of light-gray porphyritic diorite, and a diorite sill, south, east, and west of the volcano, respectively (fig. 2).

GEOCHRONOLOGY

Six samples from Sliderock Mountain volcano were dated by the $^{40}Ar/^{39}Ar$ step-heating technique. Four hornblende separates were prepared from intrusive rock samples and two sericite separates were prepared from samples of altered rock that hosts precious metal deposits at Gold Hill. Although many of the basaltic andesite lava flows contain amphibole, separates of sufficient quantity and purity could not be prepared. Samples selected for dating were crushed and sieved and mineral concentrates were prepared using standard gravimetric (heavy liquid) and magnetic techniques. Mineral separates were further purified by hand-picking. Separates were sealed in silica vials and irradiated in the central thimble of the U.S. Geological Survey TRIGA reactor for 30 hours. Neutron flux during irradiation was monitored using hornblende standard MMhb-1, which has a K-Ar age of 520.4±1.7 Ma (Samson and Alexander, 1987).

After irradiation, the samples were progressively degassed in a double-vacuum resistance furnace in a series of nine to sixteen 20-minute-long steps to a maximum temperature of 1600°C. Apparent ages were calculated using decay constants recommended by Steiger and Jäger (1977). The determination of whether the individual apparent ages yielded a "plateau" was made using the critical value test of Dalrymple and Lanphere (1969) following the plateau definition of Fleck and others (1977). Plateau dates were calculated using a weighted mean, where weighting is by the inverse of the analytical variance (Taylor, 1982). A detailed description of analytical procedures similar to those used in this study is given by Tysdal and others (1990, App. 1). Results of $^{40}Ar/^{39}Ar$ are presented as age spectra and apparent $^{39}Ar/^{37}Ar$ ratios (fig. 4); analytical data are shown in table 1.

Two samples of the diorite and granodiorite stock of Sliderock Mountain stock were dated. Sample nos. 202109 and 91SR2b gave total gas dates of 78.5±0.5 and 81.3±0.6 Ma (2σ), respectively. With the exception of low temperature steps, both samples have relatively constant $^{39}Ar/^{37}Ar$ ratios for more than about 90 percent of the potassium-derived ^{39}Ar ($^{39}Ar_K$) released (fig. 4*A*), which indicates that a single homogeneous phase was degassed at higher temperatures during step-heating experiments. Amphibole sample no. 91SR2b has a strongly U- or saddle-shaped age spectrum (fig. 4*A*) characterized by anomalously old apparent ages in the low- and high-temperature steps and younger apparent ages for intermediate temperature steps (fig. 4*A*). Such a spectrum is characteristic of the incorporation of excess ^{40}Ar, a phenomenon common in plutonic amphibole (Lanphere and Dalrymple, 1976). Because the sample may have incorporated excess ^{40}Ar, a maximum age is given by the minimum age defined by the intermediate temperature steps; in this case, the age of the hornblende must be less than about 77.4 Ma. Because the shape of the age spectrum is suggestive of the presence of excess ^{40}Ar, we analyzed the data using a $^{39}Ar/^{40}Ar$ versus $^{36}Ar/^{40}Ar$ inverse correlation diagram (McDougall and Harrison, 1988). In contrast to the apparent ages calculated for individual temperature steps in age spectrum diagrams, correlation analysis makes no assumption regarding the initial $^{40}Ar/^{36}Ar$ ratio of the sample. The $^{39}Ar/^{40}Ar$ versus $^{36}Ar/^{40}Ar$ data for sample no. 91SR2b (fig. 5) scatter about a line (mean square of weighted deviates, MSWD, is 6.9) that defines an apparent age of 77.4 (N = 9/11 steps). The analytical error for the regression (±0.19 Ma, 1σ) has been adjusted to account for an external error component in the regression by multiplying

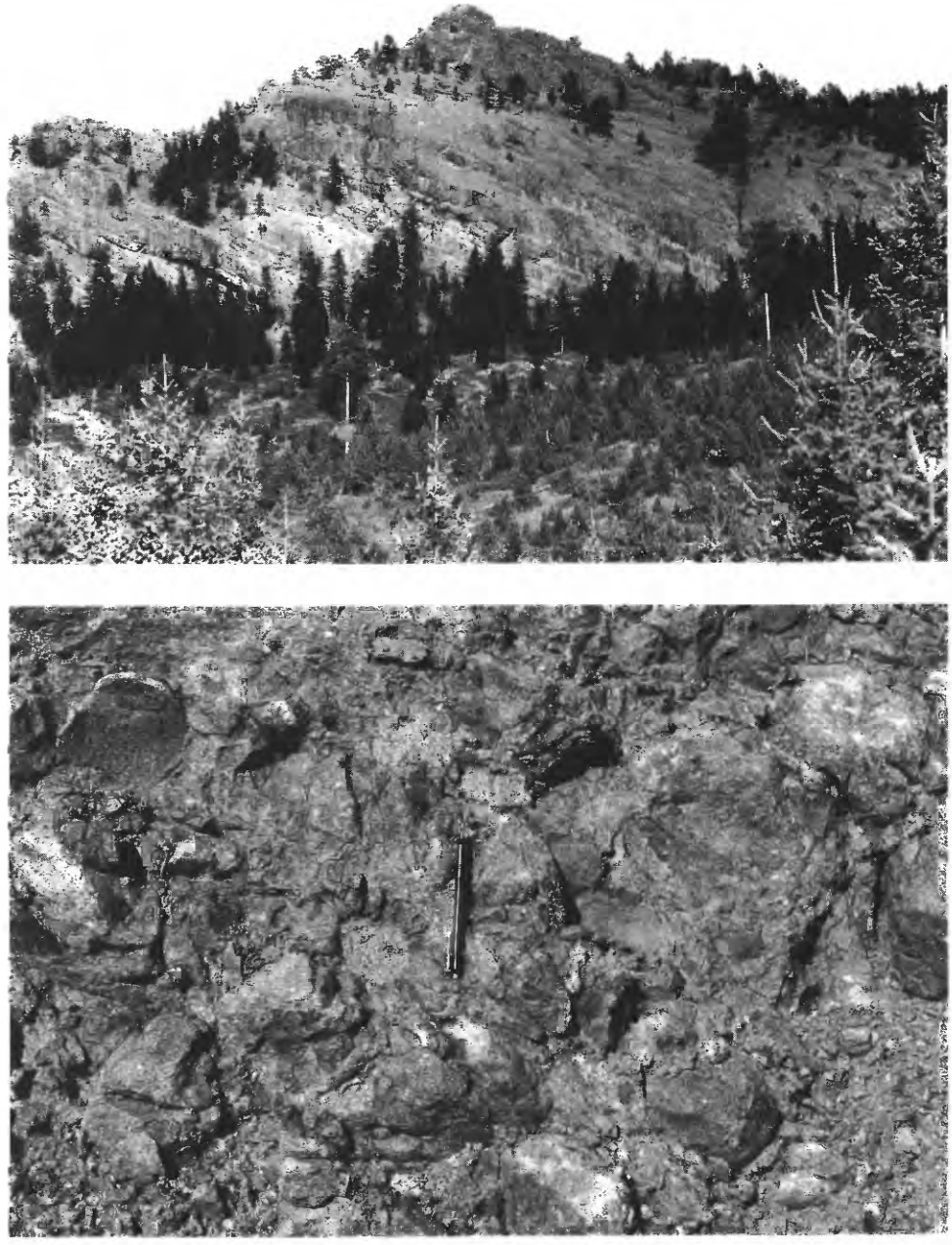

Figure 3. Photographs of Sliderock Mountain stratovolcano lahars. *A*, Individual mudflows are massive and tens of meters thick; bedding is absent or poorly developed in most places. *B*, Close-up view of clast-supported lahar; clasts are composed of disaggregated basaltic andesite lava, whereas matrix is composed of ash and finely comminuted lava.

the observed error by the square root of the MSWD to account for the excess scatter in the regression (Ludwig, 1988) and yields a more appropriate estimate of the analytical error of ±1.0 Ma (2σ). The initial $^{40}Ar/^{36}Ar$ ratio determined from the regression is 497±13 (2σ), which is significantly greater than the atmospheric value of 295.5. The high initial $^{40}Ar/^{36}Ar$ ratio clearly indicates that this sample contains excess ^{40}Ar. Therefore, we consider the age determined by the correlation diagram to be the most reliable estimate for the age of sample no. 91SR2b.

Sample no. 202109 has a similarly discordant age spectrum (fig. 4*A*), suggestive of excess ^{40}Ar incorporation, but the sample may have also experienced minor ^{40}Ar loss. The age spectrum for this sample has two steps that overlap and yield an apparent plateau with an age of 77.70±0.24 Ma, but this age may be misleading because greater than 60 percent of the $^{39}Ar_K$ was released in a single temperature step at 1150°C. Degassing most of the $^{39}Ar_K$ in a single step precludes resolution of the fine detail of the age spectrum. Analysis of the $^{40}Ar/^{39}Ar$ data using a correlation diagram gives an apparent age of 77.97±0.12 Ma (N=8/11 steps, MSWD=2.19), with an initial $^{40}Ar/^{36}Ar$ ratio of 313±5, which is somewhat greater than the present-day atmospheric value.

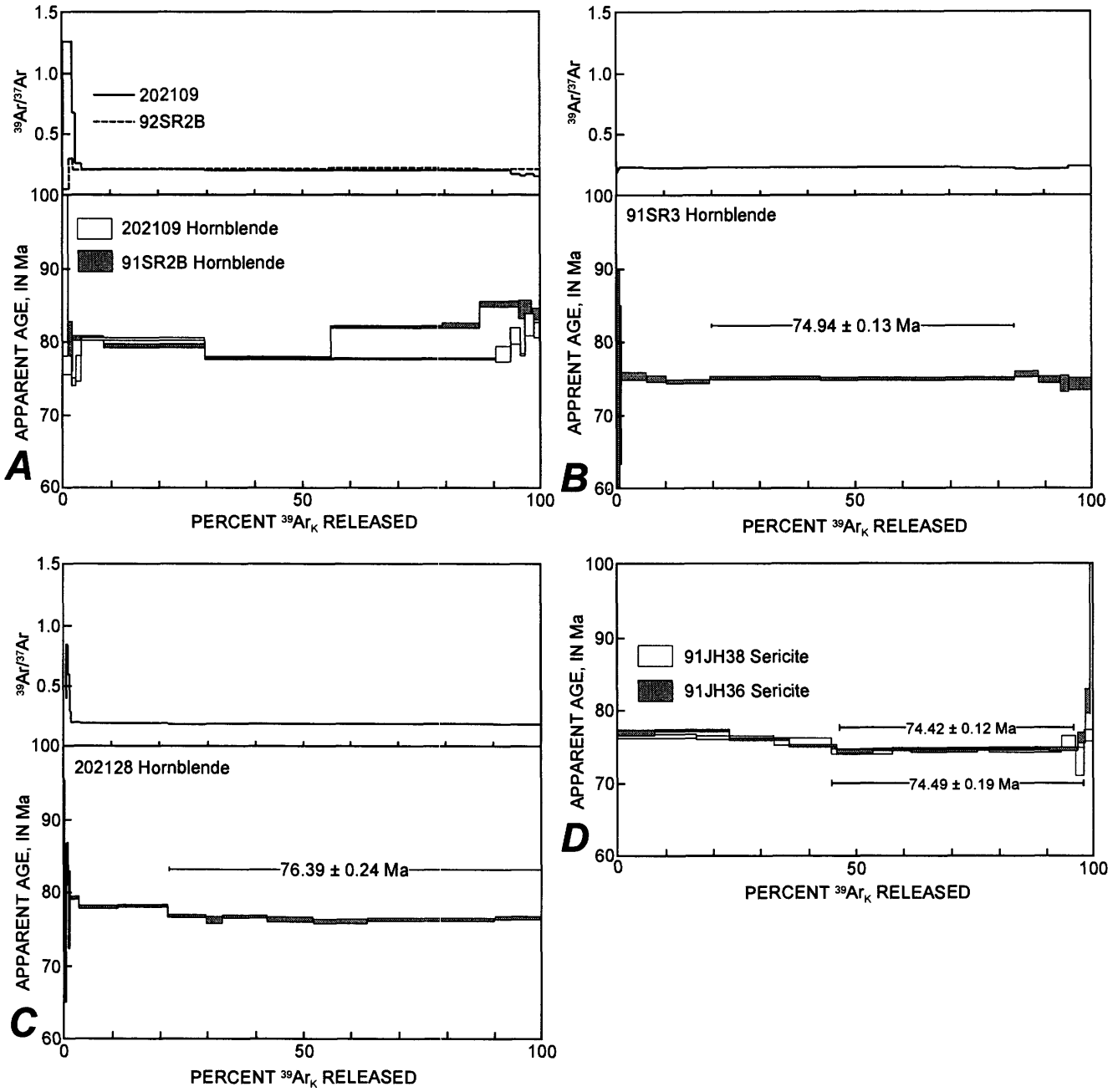

Figure 4. $^{40}Ar/^{39}Ar$ age spectra and $^{39}Ar/^{37}Ar$ ratios for samples from Sliderock Mountain volcano. *A*, hornblende from the Sliderock Mountain stock; *B*, hornblende from hornblende dacite of the Lodgepole intrusion; *C*, hornblende from an andesite dike; and *D*, sericite from altered rock associated with gold-bearing veins in the Sliderock Mountain stock. The height of rectangles for individual temperature steps in age spectra represent analytical error at ±1σ; mean ages are given at ±2σ.

Combining the two correlation ages from sample nos. 91SR2b and 202109 yields an arithmetic mean of 77.78±0.57 Ma (2σ; error based on the standard error of the mean) (Taylor, 1982), which may be a reasonable estimate for the closure age for ^{40}Ar diffusion from hornblende in the stock of Sliderock Mountain. However, this type of simple average makes no provision for the quality or precision of the analyses and is strictly appropriate only in cases where the analytical errors for the age determinations are equal in magnitude or are unknown. In this case, however, the analytical errors between the two correlation ages are significantly different. Where analytical errors are unequal, ages may be calculated using a weighted mean, where weighting is by the inverse of the analytical variance (Taylor, 1982). By utilizing this method, a measure of the "reliability" of each age measurement is incorporated in determining the best estimate of the age of the sample (Fleck and others, 1996). Calculating a weighted mean for these samples gives

Table 1. $^{40}Ar/^{39}Ar$ incremental heating data for samples from Sliderock Mountain stratovolcano, Montana.

[$^{40}Ar_R$ is radiogenic ^{40}Ar in volts signal; $^{39}Ar_K$ is potassium-derived ^{39}Ar in volts signal; $^{40}Ar_R/^{39}Ar_K$ is the ratio of $^{40}Ar_R$ to $^{39}Ar_K$ after correction for mass-discrimination and interfering isotopes; $^{39}Ar/^{37}Ar$ is the ratio of $^{39}Ar_K$ to $^{37}Ar_{Ca}$ (this value can be converted to the approximate K/Ca by multiplying by 0.52); $\%^{40}Ar_K$ and $\%^{39}Ar$ are the percent of radiogenic ^{40}Ar and percent of total ^{39}Ar released in each temperature step. Temperature steps in boldface are those used in the calculation of plateau age. Conversion of volts signal to moles Ar can be made using a conversion factor of 1.252×10^{-12} moles argon per volt of signal]

Temp (°C)	$^{40}Ar_R$	$^{39}Ar_K$	$^{40}Ar_R/^{39}Ar_K$	$^{39}Ar/^{37}Ar$	$\%^{40}Ar_R$	$\%^{39}Ar$	Apparent Age (Ma at 1σ)
Sample no. 202109: Hornblende; 193.1 mg; J-value = 0.009420 ±0.1% (1σ)							
900	0.01536	0.00371	4.138	0.51	14.2	0.2	69.0 ± 2.8
1000	0.20430	0.04428	4.614	1.26	38.8	1.9	76.75 ± 1.30
1100	0.06617	0.01479	4.474	0.67	42.7	0.6	74.46 ± 0.50
1200	0.13035	0.02843	4.585	0.25	56.5	1.2	76.28 ± 1.76
1300	2.9085	0.60173	4.834	0.20	91.8	25.8	80.32 ± 0.16
1350	6.6463	1.4226	4.672	0.20	96.4	61.0	77.70 ± 0.12
1375	0.35900	0.07625	4.708	0.20	82.1	3.3	78.29 ± 1.05
1400	0.20929	0.04301	4.866	0.17	76.5	1.8	80.85 ± 1.13
1425	0.12769	0.02713	4.707	0.15	70.1	1.2	78.27 ± 0.12
1500	0.22140	0.04463	4.960	0.17	74.7	1.9	82.38 ± 1.53
1600	0.13081	0.02662	4.913	0.15	52.0	1.1	81.62 ± 0.95
Total Gas			4.723				78.53 ± 0.25
Sample no. 91SR2B: Hornblende; 148.5 mg; J-value = 0.005230 ±0.2% (1σ)							
750	0.23788	0.01529	15.556	0.05	24.9	1.2	141.1 ± 1.6
850	0.09930	0.01155	8.598	0.30	60.0	0.9	79.4 ± 3.4
950	0.69813	0.07999	8.728	0.21	86.4	6.3	80.52 ± 0.35
1000	2.3118	0.26869	8.604	0.22	95.3	21.1	79.40 ± 0.18
1033	2.8069	0.33317	8.425	0.22	96.4	26.2	77.79 ± 0.18
1066	2.6447	0.29739	8.893	0.22	96.8	23.4	82.01 ± 0.19
1100	0.90993	0.10214	8.909	0.22	89.4	8.0	82.16 ± 0.38
1150	0.96318	0.10429	9.236	0.21	95.1	8.2	85.10 ± 0.39
1200	0.33431	0.03652	9.154	0.21	90.4	2.9	84.36 ± 1.27
1300	0.21151	0.02329	9.082	0.21	81.6	1.8	83.72 ± 0.81
Total Gas			8.817				81.32 ± 0.28
Sample no. 202128: Hornblende; 244.8 mg; J-value = 0.007388 ±0.2% (1σ)							
700	0.03128	0.00414	7.564	0.43	2.7	0.1	98.1 ± 0.5
800	0.10994	0.01504	7.308	0.39	13.9	0.5	94.9 ± 0.5
850	0.03248	0.00644	5.041	0.83	8.8	0.2	66.0 ± 1.0
900	0.03393	0.00542	6.261	0.82	11.4	0.2	81.6 ± 4.9
950	0.03779	0.00587	6.436	0.59	6.2	0.2	83.8 ± 3.0
1000	0.05113	0.00859	5.950	0.28	5.4	0.3	77.6 ± 5.2
1025	0.37415	0.06157	6.077	0.20	18.8	2.0	79.23 ± 0.21
1050	1.5309	0.25624	5.974	0.19	36.1	8.2	77.92 ± 0.21
1075	1.9253	0.32128	5.992	0.19	39.1	10.2	78.15 ± 0.18
1100	1.4448	0.24564	5.882	0.18	48.9	7.8	76.74 ± 0.18
1125	0.63996	0.10970	5.834	0.18	92.9	3.5	76.12 ± 0.44
1150	1.7220	0.29311	5.875	0.19	94.6	9.3	76.65 ± 0.18
1200	1.7792	0.30443	5.844	0.19	93.6	9.7	76.26 ± 0.29
1250	2.0763	0.35655	5.823	0.19	93.6	11.4	75.99 ± 0.23
1350	4.8678	0.83383	5.838	0.19	95.8	26.6	76.18 ± 0.22
1450	0.31048	0.31048	5.855	0.18	95.7	9.9	76.39 ± 0.27
Total Gas			5.887				76.8 ± 0.3

an apparent age of 77.96±0.24 Ma (2σ). Although analytically very precise, the geologic significance of this age must be viewed with caution because the correlation ages may also represent maximum apparent ages. In addition, the high analytical precision of the age is probably geologically unrealistic because the contribution of the sample no. 91SR2b age to the calculated mean is minor owing to its large analytical error (Taylor, 1982). Given the problematic nature of the analyzed samples due to the presence of such things as excess ^{40}Ar and scatter in the isochrons, the quoted uncertainties of either mean age probably should be viewed as minimum values. Because of the magnitude of the adjusted analytical error from the regression of sample no. 91SR2b correlation data, we consider a reasonable and conservative estimate for the mean hornblende age from the stock of Sliderock Mountain to be about 78±1 Ma (based on the

Table 1. $^{40}Ar/^{39}Ar$ incremental heating data for samples from Sliderock Mountain stratovolcano, Montana—Continued.

Temp (°C)	$^{40}Ar_R$	$^{39}Ar_K$	$^{40}Ar_R/^{39}Ar_K$	$^{39}Ar/^{37}Ar$	$\%^{40}Ar_R$	$\%^{39}Ar$	Apparent Age (Ma at 1σ)
Sample no. 91SR3: Hornblende; 215.6 mg; J-value = 0.007450 ±0.2% (1σ)							
600	0.1885	0.00436	4.325	0.28	15.5	0.1	57.2 ± 12.4
700	0.01554	0.00342	4.544	0.19	17.2	0.1	60.1 ± 8.5
800	0.03290	0.00544	6.045	0.18	10.6	0.2	79.5 ± 11.5
850	0.01058	0.00491	2.155	0.20	13.8	0.2	29 ± 18
900	0.03146	0.00550	5.715	0.21	49.6	0.2	75.2 ± 8.2
950	0.03465	0.00616	5.621	0.23	51.7	0.2	74.0 ± 10.8
1000	0.89419	0.15642	5.717	0.23	81.5	5.0	75.24 ± 0.48
1025	0.74029	0.13013	5.869	0.22	85.0	4.2	74.88 ± 0.47
1050	1.6597	0.29333	5.658	0.22	90.9	9.4	74.49 ± 0.24
1075	4.1423	0.72681	5.699	0.22	93.5	23.3	75.02 ± 0.13
1100	5.3529	0.94074	5.690	0.22	92.8	30.2	74.90 ± 0.11
1125	1.8898	0.33198	5.692	0.22	88.8	10.7	74.93 ± 0.11
1150	0.90664	0.15784	5.744	0.21	89.9	5.1	75.59 ± 0.34
1200	0.79238	0.13950	5.680	0.21	92.0	4.5	74.77 ± 0.43
1250	0.32979	0.05843	5.644	0.22	88.6	1.9	74.30 ± 1.10
1450	0.84325	0.14961	5.636	0.24	92.4	4.8	74.21 ± 0.80
Total Gas			5.681				74.78 ± 0.39
Sample no. 91JH38: Sericite; 68.5 mg; J-value = 0.007365 ±0.1% (1σ)							
600	1.8195	0.30732	5.920	188.2	91.0	7.8	76.82 ± 0.32
700	3.6868	0.62046	5.942	129.9	96.5	15.7	77.10 ± 0.12
750	2.8953	0.49511	5.848	185.3	96.5	12.5	75.94 ± 0.12
800	2.3084	0.39982	5.774	181.5	97.4	10.1	74.96 ± 0.18
850	1.7335	0.30300	5.721	191.2	94.6	7.6	74.29 ± 0.18
900	1.7307	0.30192	5.732	128.3	95.6	7.6	74.43 ± 0.17
950	3.2692	0.57114	5.724	291.5	95.9	14.4	74.33 ± 0.11
1000	3.3670	0.58675	5.738	246.9	95.6	14.8	74.50 ± 0.11
1050	1.4341	0.24980	5.741	140.1	93.7	6.3	74.54 ± 0.18
1100	0.36108	0.06160	5.862	71.64	87.6	1.6	76.08 ± 0.69
1150	0.21684	0.03459	6.269	17.76	83.3	0.9	81.2 ± 1.7
1350	0.23697	0.03054	7.760	7.04	70.2	0.8	100.0 ± 2.3
Total gas			5.820				75.55 ± 0.18
Sample no. 91JH36: Sericite; 35.6 mg; J-value = 0.00740 ±0.1% (1σ)							
700	3.4148	0.58333	5.854	171.2	92.8	16.5	76.33 ± 0.26
800	3.4022	0.58297	5.836	164.2	95.8	16.5	76.10 ± 0.21
900	2.4473	0.42229	5.795	132.0	96.9	11.9	75.58 ± 0.47
950	2.6193	0.46031	5.690	150.1	95.6	13.0	74.24 ± 0.26
1000	4.0817	0.71448	5.713	272.4	97.0	20.2	74.53 ± 0.11
1050	3.0832	0.54029	5.707	181.6	96.6	15.3	74.45 ± 0.34
1100	0.66482	0.11507	5.778	65.27	95.6	3.2	75.36 ± 0.91
1150	0.32443	0.05811	5.583	23.19	90.8	1.6	72.87 ± 1.89
1350	0.37944	0.06473	5.862	11.32	91.4	1.8	76.44 ± 0.70
Total gas			5.765				75.20 ± 0.31

magnitude of the error from sample no. 91SR2b). Given the high closure temperature for ^{40}Ar diffusion in hornblende (500°±50°C) (McDougall and Harrison, 1988), coupled with the fact that this hypabyssal stock intrudes overlying, cogenetic volcanic rocks and therefore probably cooled quite rapidly, the dates probably closely approximate the emplacement age of the stock.

Sample no. 202128 is a porphyritic biotite-hornblende dacite from the Lodgepole intrusion (Brozdowski, 1983), a laccolith about 5 km south of Sliderock Mountain volcano in Clover Basin (figs. 1, 2). The Lodgepole intrusion is compositionally similar to intrusive rocks in the core of the Sliderock Mountain volcano and lithologically similar clasts are present in some lahars of Sliderock Mountain volcano. Hornblende from the Lodgepole intrusion gave a total gas age of 76.80±0.50 Ma. Although the spectrum for sample no. 202128 indicates an excess ^{40}Ar component in low temperature steps, it is simply interpreted (fig. 4*C*), giving a plateau age of 76.39±0.24 Ma for 78.2 percent of the $^{39}Ar_K$ released. The $^{39}Ar/^{37}Ar$ ratio for this interval is relatively constant, which indicates that a single phase was degassed during this heating interval.

Hornblende from one of the radial andesite dikes (sample no. 91SR3) that is representative of the dike swarm gave a total gas date of 74.8±0.8 Ma. Overall, the age spectrum is simple in that individual temperature steps give essentially identical apparent ages and have similar $^{39}Ar/^{37}Ar$ ratios over virtually the entire range of $^{39}Ar_K$ released (fig. 4*C*). A weighted-mean plateau date for the 1075° to 1125°C steps (64.2 percent of the $^{39}Ar_K$ released) gives an age of 74.94±0.13 Ma.

Finally, two sericite samples (sample nos. 91JH36 and 91JH38) associated with potassically altered rock that surrounds a gold vein in the Gold Hill mine area were dated. Both sericite spectra show initial apparent ages of about 77 Ma; apparent ages decrease in higher temperature steps, have relatively constant apparent ages of about 74.5 Ma in intermediate temperature steps, and increase in the highest temperature steps (fig. 4*D*). Overall, these spectra are indicative of excess ^{40}Ar, although the high radiogenic yield of the samples combined with limited spread in $^{36}Ar/^{40}Ar$ ratios precluded precise determinations of initial $^{40}Ar/^{36}Ar$ values using correlation diagrams. The two samples yield similar plateau dates of 74.42±0.12 Ma and 74.49±0.19 Ma. Because the samples are from the same vein and give essentially identical dates, we calculated a weighted-mean age of 74.44±0.20 Ma and consider this to be the best estimate for the age of potassic alteration.

The $^{40}Ar/^{39}Ar$ dating described here indicates that the Sliderock Mountain stock is probably less than about 78 to 77 Ma, although an absolute age is difficult to quantify given the effect of excess ^{40}Ar on the samples. If the stock is approximately coeval with the nearby Lodgepole intrusion, it could be as young as about 76.5 Ma. Alternatively, the compositionally similar intrusion may represent a slightly younger igneous event. Because the stock cuts the volcaniclastic and volcanic strata, their age is somewhat greater. Although it is not possible to precisely establish the age, an approximate age of about 78±1 Ma is what we consider to be a reasonable maximum age estimate for the initiation of volcanism and intrusive activity at the Sliderock Mountain volcano. Final magmatic activity is represented by the emplacement of radial dikes, which intrude all other phases of the volcano, at about 74.9 Ma. The $^{40}Ar/^{39}Ar$ dates of about 74.4 Ma from hydrothermally altered phases of the stock indicate that weak precious mineralization was probably genetically related to the stock and occurred during the final phases of igneous activity at Sliderock Mountain volcano.

The 78 to 75 Ma dates for igneous activity at Sliderock Mountain volcano are somewhat younger than the 82.4±4.1 and 81.8±3.1 Ma (both at 1σ) K-Ar dates previously reported for rocks in the Sliderock Mountain area (Marvin and Dobson, 1979). The apparent ages of these conventional K-Ar dates may have been influenced by the excess ^{40}Ar we observed during the course of our study. Our $^{40}Ar/^{39}Ar$ dates are similar to conventional K-Ar dates for the Elkhorn Mountains Volcanics and volcanic rocks in the Maudlow basin north and west of the Crazy Mountains Basin (Robinson and Marvin, 1967; Robinson and others, 1968; Tilling and others, 1968; Hanna, 1973; Marvin and others, 1989). Additional isotopic dating is necessary elsewhere throughout the volcanic field in order to more accurately constrain the ages of Late Cretaceous magmatism along the southern margin of the Crazy Mountains Basin and to relate magmatism to the regional tectono-magmatic evolution of the northern Rocky Mountains.

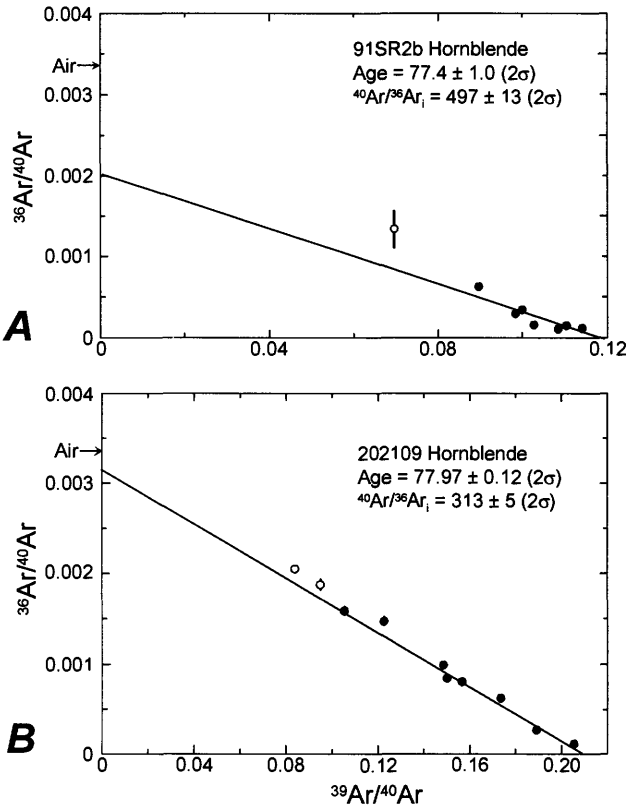

Figure 5. $^{39}Ar/^{40}Ar$ versus $^{36}Ar/^{40}Ar$ correlation diagrams for two hornblende separates from the stock of Sliderock Mountain. Circles represent $^{39}Ar/^{40}Ar$ versus $^{36}Ar/^{40}Ar$ ratios determined for each temperature step; lines about the points represent the error in the ratios at one standard deviation. For most steps, the errors on the ratios are smaller than the size of the symbols. Closed circles are those points used in the regression; open circles are those rejected. Individual points were rejected based on significantly different $^{39}Ar/^{40}Ar$ versus $^{36}Ar/^{40}Ar$ ratios or because of significantly different $^{39}Ar/^{37}Ar$ ratios (table 1) which suggest that the gas evolved from these steps during the step-heating experiment may be due to a different mineral phase. $^{40}Ar/^{36}Ar_i$ is the initial $^{40}Ar/^{36}Ar$ value as determined from the inverse of the $^{36}Ar/^{40}Ar$ intercept. *A*, sample no. 91SR2b; one of the points is not shown because it plots off the scale of the correlation diagram. *B*, sample no. 202109.

PETROGRAPHY

Basaltic andesite lava flows of Derby Ridge are composed of light-gray to light-olive gray intersertal rocks that are weakly trachytically layered in some places. Crystal abundances in these rocks are highly variable; phenocrysts are subhedral to euhedral laths of zoned and albite-twinned plagioclase (0.6 mm) altered to clay, subhedral grains of pale-green clinopyroxene (0.5 mm), and anhedral grains of opaque oxide minerals (0.2 mm). Accessory minerals include apatite and hornblende. The groundmass, partly altered to calcite in some places, is composed of a very fine grained, turbid intergrowth of plagioclase and opaque oxide minerals; some rocks contain incipiently devitrified glass.

Light- to dark-gray basaltic andesite lava flows that overlay the lahar deposits have highly variable crystal contents; phenocrysts are subhedral to euhedral laths of albite-twinned and zoned plagioclase (0.6 mm), subhedral clinopyroxene (0.5 mm), and anhedral opaque oxide minerals (0.2 mm). The groundmass is a devitrified intergrowth of fine-grained plagioclase and opaque oxide minerals. The lava flows are characterized by an intersertal texture; trachytic layering is present locally.

The core of the volcano is composed of very light gray to medium-gray, hypidiomorphic granular diorite to granodiorite. This rock is principally composed of subhedral to euhedral laths of zoned and albite-twinned plagioclase (0.8 mm) that is moderately to strongly sericitized. Hornblende (0.8 mm) is the principal mafic mineral and forms straw-yellow to olive-green subhedral laths. About 5 percent of the crystals in the stock are anhedral grains of opaque oxide minerals (0.2 mm). Quartz (anhedral, very fine grained, and interstitial), biotite, or clinopyroxene are present in some samples; apatite is a ubiquitous trace phase. The stock is texturally heterogeneous and is characterized by pronounced grain size variation; it is fine grained in most places but is locally medium grained. The groundmass in some samples is a turbid intergrowth of very fine grained plagioclase, chlorite, calcite, and opaque oxide minerals.

The basaltic trachyandesite to trachyte dikes contain 15–30 percent phenocrysts, including euhedral to subhedral laths of strongly zoned, albite-twinned, clay-altered plagioclase (1 mm) and subequal amounts of anhedral to subhedral pale-green clinopyroxene (0.5 mm) and subhedral to euhedral olive-green hornblende (1 mm); apatite is a trace mineral. The groundmass is a turbid, devitrified intergrowth of plagioclase and opaque oxide minerals; secondary zeolite minerals are common. Three small intrusions (du Bray and others, 1994), probably related to the dikes, are porphyritic and contain 25–40 percent phenocrysts of plagioclase, hornblende, and biotite; calcite and zeolite minerals are secondary minerals in the fine-grained groundmass and replace plagioclase.

GEOCHEMISTRY

Geochemical analyses were obtained for 26 samples of the Sliderock Mountain stratovolcano. All analyses were performed in the laboratories of the U.S. Geological Survey in Denver, Colorado. Major oxide analyses were performed (analysts, D.F. Siems, J.E. Taggart, and J.S. Mee) using X-ray fluorescence techniques (Taggart and others, 1987). The ratios Fe^{2+}: total iron as Fe^{2+} were adjusted to 0.85 and major oxide abundances recalculated to 100 percent, on an anhydrous basis. Trace element abundances were determined (by E.A. du Bray) by energy-dispersive X-ray fluorescence spectroscopy (Elsass and du Bray, 1982) using ^{109}Cd and ^{241}Am radio-isotope excitation sources; the accuracy of this data is quantified by Yager and Quick (1992).

Rocks of the Sliderock Mountain stratovolcano are subalkaline to transitionally alkaline (table 2, fig. 6). Compositions of the lava flows stratigraphically above and below the lahar deposits, and most of the dikes, are indistinguishable (fig. 7) and cluster in the basaltic andesite and basaltic trachyandesite fields (Le Bas and others, 1986); some lava flow compositions extend to andesite or trachyandesite and one dike is composed of trachyte. Compositions of intrusive rocks from Sliderock Mountain stratovolcano are bimodally distributed. About half of these have compositions of

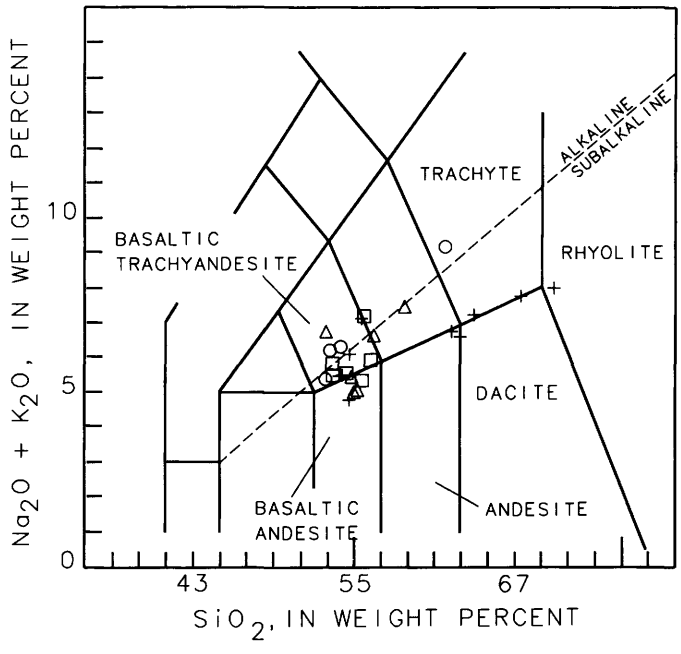

Figure 6. Total alkali-silica variation diagram with IUGS classification grid (Le Bas and others, 1986) showing analyses of samples from the Sliderock Mountain stratovolcano (table 2). Alkaline-subalkaline divider is that of Irvine and Baragar (1971). Data are plotted as follows: intrusive phase, plus signs; dikes, circles; basaltic andesite lava flows of Derby Ridge, triangles; and basaltic andesite lava flows deposited atop the lahar deposits, squares.

Table 2. Chemical compositions of samples from the Sliderock Mountain stratovolcano, Montana.

[Major oxide analyses (weight percent) normalized to 100 percent, volatile free. FeO/FeO* recalculated to 0.80. All trace element data are in parts per million. Sum_i, original, pre-normalization total with total iron as Fe_2O_3. LOI, loss on ignition; bdl, below detection limit]

	Basaltic andesite lava flows of Derby Ridge						Basaltic andesite lava flows						Stock
Sam. No.--	202112	202114	202115	202116	202124	202125	202091	202092	202093	202100	202119	202120	202094
SiO_2	54.76	56.47	58.75	52.85	54.99	55.27	55.58	53.30	55.66	54.35	53.39	56.21	54.65
Al_2O_3	19.81	19.25	17.94	19.48	19.04	19.07	19.38	17.66	18.90	19.24	18.93	18.26	18.79
Fe_2O_3	1.14	1.08	1.01	1.06	1.31	1.19	1.12	1.42	1.20	1.24	1.31	1.26	1.23
FeO	5.80	5.52	5.15	5.42	6.67	6.07	5.73	7.26	6.11	6.30	6.70	6.40	6.28
MgO	3.11	2.79	2.79	2.52	3.51	2.97	3.17	3.79	3.14	3.16	3.95	2.90	3.90
CaO	8.88	7.15	5.80	10.72	8.20	9.28	8.61	9.13	6.49	8.94	8.97	7.73	9.24
Na_2O	3.22	3.16	4.45	4.59	2.49	2.92	3.12	3.12	3.71	3.22	3.29	3.20	2.73
K_2O	2.18	3.44	2.99	2.16	2.52	2.10	2.19	2.69	3.44	2.34	2.16	2.70	2.02
TiO_2	0.47	0.50	0.59	0.45	0.62	0.52	0.50	0.90	0.72	0.59	0.68	0.71	0.61
P_2O_5	0.48	0.51	0.40	0.51	0.50	0.48	0.46	0.56	0.52	0.49	0.48	0.50	0.43
MnO	0.16	0.14	0.12	0.24	0.15	0.14	0.14	0.15	0.12	0.15	0.14	0.12	0.13
LOI	1.18	4.16	2.11	5.97	4.96	6.96	1.26	1.84	2.86	1.14	1.61	1.45	5.53
Sum_i	100.25	99.31	99.61	99.43	99.67	99.86	99.95	100.00	99.81	100.08	99.55	99.63	99.87
Rb	51	88	73	64	56	50	63	45	66	55	45	62	51
Sr	841	652	653	860	858	795	834	971	974	941	861	803	851
Y	23	12	17	7	20	12	22	32	29	15	16	28	15
Zr	80	92	146	68	100	71	84	169	158	93	57	143	72
Nb	5	9	12	8	8	4	10	9	9	9	7	8	7
Pb	bdl	16	bdl	17	bdl	17	10	bdl	24	27	6	bdl	5
Th	bdl	12	bdl	bdl	bdl	13	13	bdl	bdl	14	bdl	bdl	20
Ba	827	1170	1356	1078	924	836	806	1013	1723	909	892	969	859
La	30	36	28	16	20	21	24	18	32	40	32	40	33
Ce	52	61	52	72	57	46	86	67	67	72	54	65	66
Nd	22	27	15	25	15	6	24	32	42	19	26	15	20

	Diorite to granodiorite stock of Sliderock Mountain									Basaltic trachyandesite and trachyte dikes			
Sam. No.--	202095	202101	202102	202105	202109	202110	202113	202121	202129	202088	202089	202111	202126
SiO_2	55.46	62.26	53.98	69.93	62.91	67.31	54.64	63.94	54.06	61.76	53.91	53.16	52.89
Al_2O_3	18.35	17.52	19.18	16.70	17.56	16.85	19.62	17.01	18.41	17.87	19.69	19.80	20.21
Fe_2O_3	1.23	0.84	1.14	0.44	0.79	0.49	1.21	0.69	1.27	0.76	1.22	1.28	1.15
FeO	6.26	4.29	5.83	2.23	4.05	2.52	6.18	3.50	6.49	3.86	6.23	6.51	5.86
MgO	2.97	2.23	4.41	0.20	2.05	0.99	2.62	2.32	4.43	1.31	2.74	2.87	3.66
CaO	7.25	5.21	8.50	1.95	5.13	3.52	8.41	4.47	8.57	4.40	8.59	8.89	9.75
Na_2O	3.65	3.81	3.49	4.47	3.81	4.56	3.70	4.70	3.16	3.58	3.74	4.03	3.18
K_2O	3.43	2.89	2.05	3.48	2.77	3.13	2.39	2.50	2.33	5.59	2.57	2.17	2.21
TiO_2	0.76	0.51	0.50	0.39	0.50	0.35	0.57	0.49	0.68	0.48	0.62	0.58	0.44
P_2O_5	0.52	0.33	0.40	0.18	0.32	0.20	0.50	0.29	0.46	0.26	0.53	0.54	0.50
MnO	0.12	0.12	0.14	0.04	0.11	0.07	0.16	0.09	0.14	0.14	0.16	0.17	0.15
LOI	1.95	2.40	2.93	3.20	1.86	2.34	4.40	1.15	3.68	2.46	2.34	3.37	3.72
Sum_i	99.63	99.88	98.95	99.25	99.10	99.33	99.85	99.12	99.45	99.71	100.02	100.01	99.82
Rb	69	75	44	66	67	60	59	42	59	108	58	55	56
Sr	1021	940	855	650	946	1263	984	1042	845	1056	1183	832	932
Y	22	21	11	8	21	20	15	20	25	23	20	22	5
Zr	130	148	54	108	149	166	71	131	83	131	88	62	58
Nb	15	12	9	13	13	13	9	9	5	13	9	7	10
Pb	13	bdl	bdl	19	16	19	bdl	17	bdl	23	6	13	18
Th	bdl	bdl	bdl	bdl	bdl	bdl	bdl	bdl	bdl	15	bdl	bdl	bdl
Ba	1315	1560	861	2507	1681	2111	1114	1759	849	1367	883	966	810
La	40	46	15	20	31	28	25	29	36	54	31	21	15
Ce	62	51	53	32	57	70	57	52	70	70	58	57	49
Nd	46	29	16	38	33	22	27	27	22	30	35	32	23

basaltic andesite or basaltic trachyandesite, and the remainder have compositions of dacite to rhyolite.

Compositions of the analyzed samples are metaluminous; the average alumina saturation index (molar Al_2O_3/

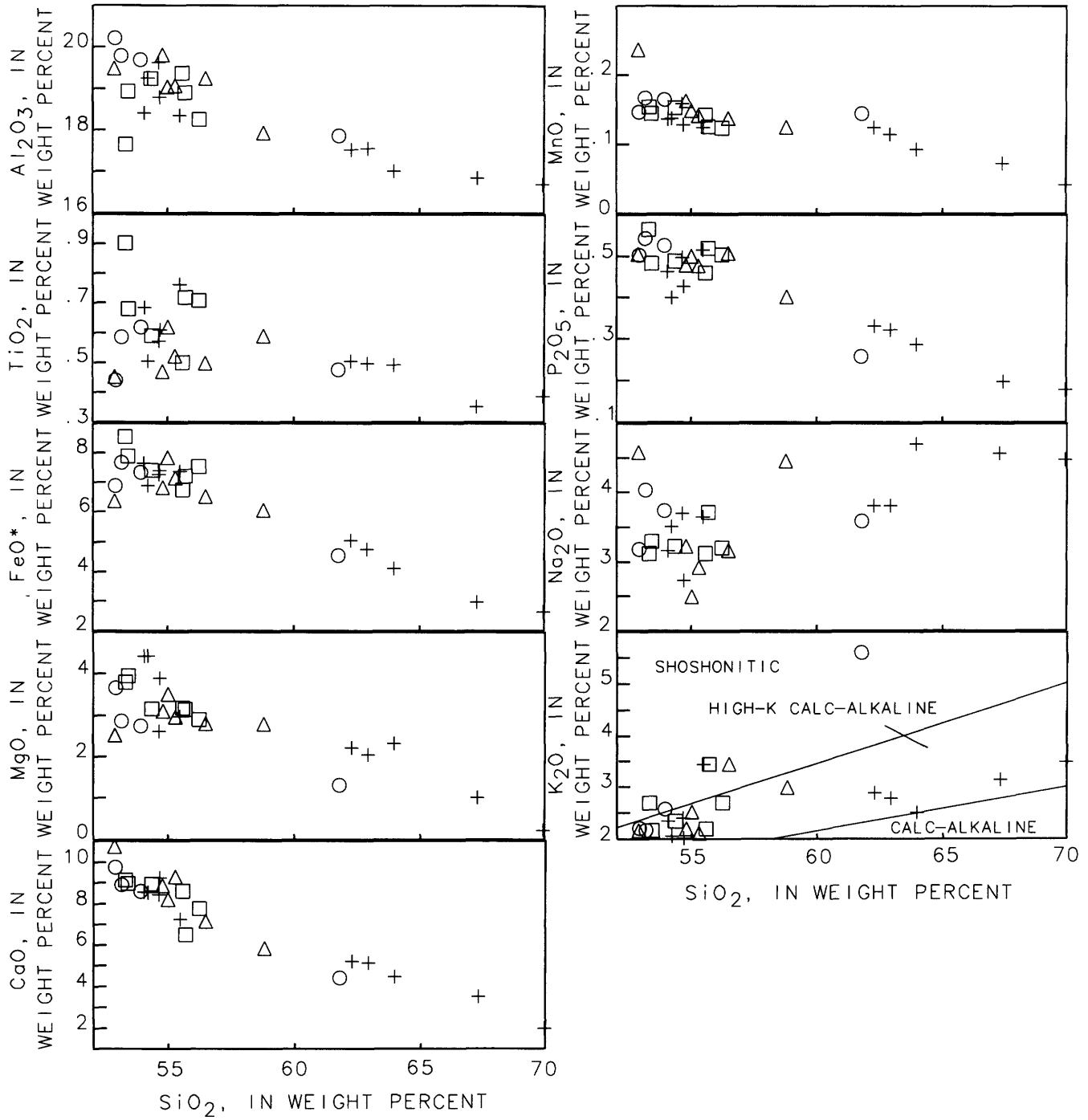

Figure 7. Variation diagrams showing abundances of major oxides in volcanic rock samples from the Sliderock Mountain stratovolcano (table 2). Discriminant lines on K_2O versus SiO_2 diagram are from Ewart (1982). See figure 6 for explanation of symbols.

[$CaO+K_2O+Na_2O$]) for the 26 samples is 0.844. This value is consistent with derivation of the volcanic and plutonic rocks from an igneous (mantle) source and precludes significant contamination of primary mantle-derived melts by assimilation of crustally derived sedimentary rocks (Chappell and White, 1992).

Major oxide abundance variations in the Sliderock Mountain volcano rocks are similar to those of most continental volcanic arc calc-alkaline igneous rocks. Total iron, Al_2O_3, MgO, CaO, P_2O_5, MnO, and TiO_2 abundances decrease with increasing SiO_2, whereas K_2O and Na_2O abundances increase with increasing SiO_2 (fig. 7). The K_2O abundances in most of these samples plot in the high-K calc-alkaline series of Ewart (1982) and Na_2O:K_2O is approximately 1.3. The composition of the Sliderock Mountain rocks are similar to those of other Late Cretaceous igneous

centers, including those of the Elkhorn Mountains Volcanics (Klepper and others, 1971) and chemically primitive (approximately 55 weight percent SiO_2) parts of the Boulder (Smedes, 1966; Tilling, 1973) and Idaho (Norman and others, 1992) batholiths, in western Montana and eastern Idaho. Particularly diagnostic features of the major oxide compositions of the Sliderock Mountain rocks are high Al_2O_3 and low MgO contents at about 55 weight percent SiO_2 (table 2, fig. 7).

Trace element abundances for samples of the stratovolcano are similar to those for other unevolved, mantle-derived magmas, including those of the more primitive parts of the Late Cretaceous Boulder (Tilling, 1973) and Idaho batholiths (Norman and others, 1992). Rubidium and Zr abundances for the Sliderock Mountain rocks are significantly lower and Sr abundances slightly higher than those for the Idaho batholith. Rubidium and Sr abundances are similar to and significantly higher, respectively, than their abundances in the primitive parts of the Boulder batholith. Rubidium abundances in samples of the stratovolcano increase slightly with decreasing Sr abundances, which is in accord with antithetic Rb-Sr abundance relations displayed by most igneous rocks (Macdonald and others, 1992). The average Rb/Sr ratio for these rocks, about 0.07, is very low. Yttrium and Ba abundances are similar to those for the Idaho batholith.

The degree of magmatic evolution displayed by rocks of the Sliderock Mountain stratovolcano is depicted by their relative Rb, K, and Sr abundances (fig. 8). Abundances of these elements are principally controlled by feldspar (Hanson, 1978); Sr and K abundances are depleted and Rb abundances are enriched, respectively, by feldspar fractionation. Thus, as feldspar fractionation and differentiation proceed, K, and to an even greater extent Rb, are concentrated in the residual liquid relative to Sr. Compositions plotting nearest the Sr apex of the Rb-K/100-Sr ternary diagram represent the least evolved magmas. Rocks of the Sliderock Mountain stratovolcano are significantly less evolved than those of other subduction-related magmatic systems, including those represented by middle Tertiary, ash-flow tuffs of southern Nevada (du Bray, 1995) and Tertiary volcanic rocks of the Andean arc (du Bray and others, 1995).

Compositions of Sliderock Mountain volcano rocks plot near the Sr apex of the Rb-K/100-Sr ternary diagram and thus imply very limited evolution by feldspar fractionation. The array of points defined by the intrusive rocks overlaps the array formed by all other components of the volcano. A sample of the intrusive phase of the volcano represents the most evolved part of the magmatic system; two lava samples and a dike sample have similar compositions, however, and indicate that magma was tapped from the Sliderock Mountain system, to form dikes and supply lava flow eruptions, during the entire cooling and compositional evolution of the system.

Pearce and others (1984) recognized that granitoid rocks generated in various tectonic settings have distinctive geochemical signatures and they developed trace-element

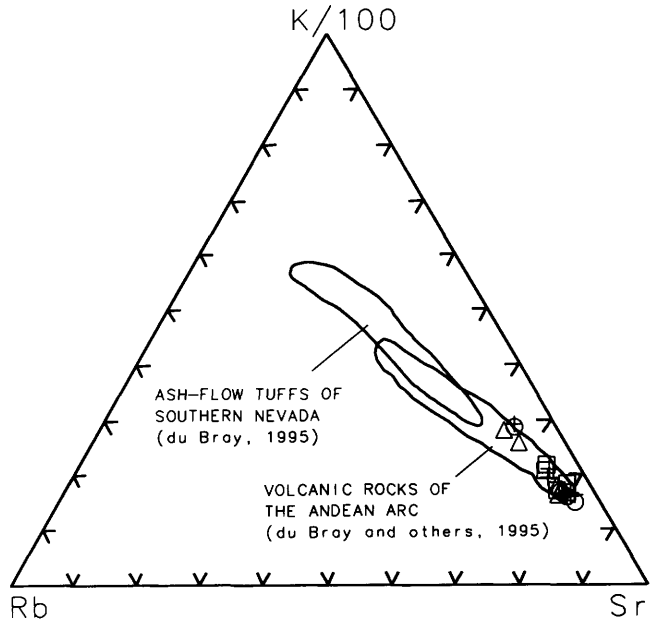

Figure 8. Ternary variation diagram showing the relative proportions of Rb, K, and Sr in samples from the Sliderock Mountain stratovolcano (table 2). See figure 6 for explanation of symbols.

discriminant diagrams from which tectonic setting can be inferred. Trace-element abundance variations in coeval volcanic and plutonic rocks generated in a given terrane should be similar. Consequently, compositions of the Sliderock Mountain rocks can be compared to the tectonic setting-trace element grids developed by Pearce and others (1984). Trace-element data for all of these samples plot in the volcanic arc field on these diagrams (fig. 9). Gill (1981) indicated that Ba/Nb ratios of modern arc rocks are greater than 26 and negative Nb anomalies on normalized extended trace element diagrams are a diagnostic geochemical characteristic of continental volcanic arc rocks. The average Ba/Nb ratio for the Sliderock Mountain rocks is about 130 and negative Nb anomalies are a ubiquitous feature of these rocks. In addition, major oxide compositions of the Sliderock Mountain rocks follow a calc-alkaline trend parallel to but displaced slightly above the Cascade trend on an AFM diagram (fig. 10). These compositional features suggest that rocks of the stratovolcano represent a subduction-related, continental volcanic arc magma system.

Compositional data for samples of the stratovolcano are characterized by several groups of oxides and elements whose abundances show mutual covariation. These covariant relations suggest that compositional variation was controlled by a distinct mineral assemblage, which is in accord with the fact that the compositions of samples of the stratovolcano form linear arrays on many variation diagrams. The minerals inferred to have influenced these compositional variations, which could have controlled the variations either by their occurrence in the partial melting residuum and (or)

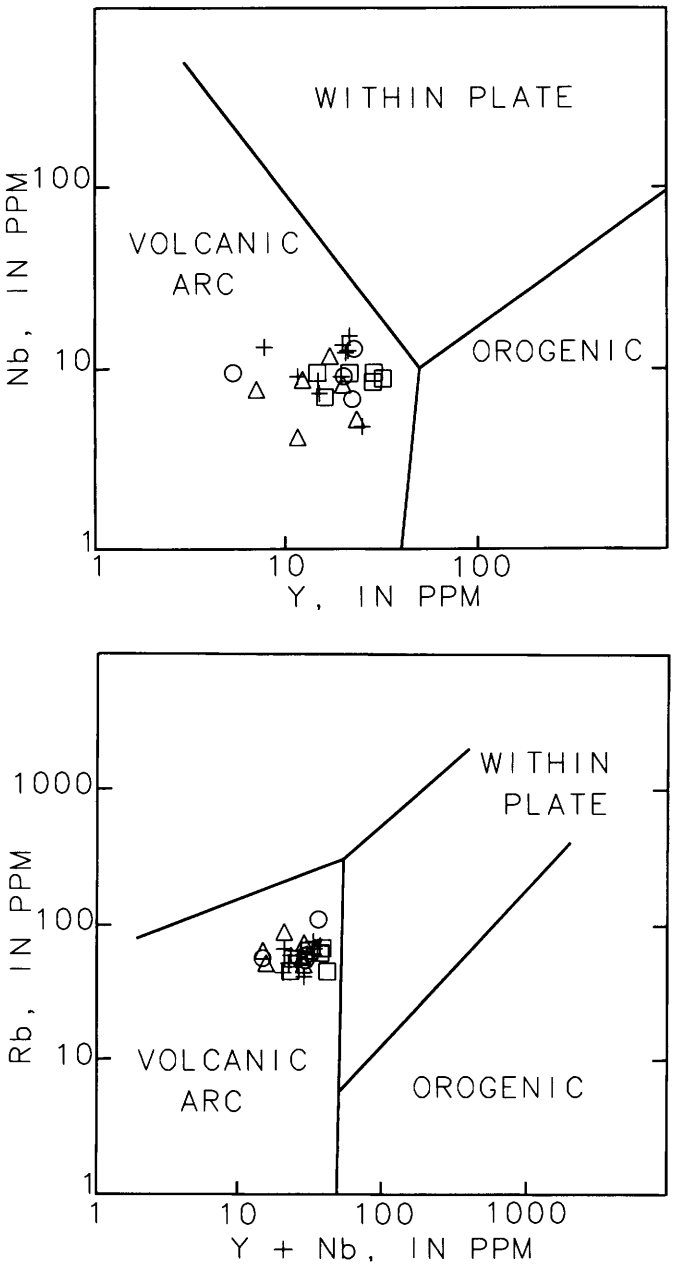

Figure 9. Trace-element tectonic-setting-discrimination variation diagrams showing compositions of volcanic rock samples from the Sliderock Mountain stratovolcano (table 2). Tectonic setting-composition boundaries from Pearce and others (1984). See figure 6 for explanation of symbols. *A*, niobium versus yttrium. *B*, rubidium versus yttrium plus niobium.

in crystal fractionation assemblages, occur as phenocrysts in the rocks.

The oxides whose abundances are most highly correlated are FeO, CaO, MgO, and Al_2O_3. Correlation coefficients (r^2) between pairs of these elements are all greater than 0.70; most are greater than 0.8 and some exceed 0.9. Mutual abundance covariations involving these oxides indicate that clinopyroxene had a major influence on

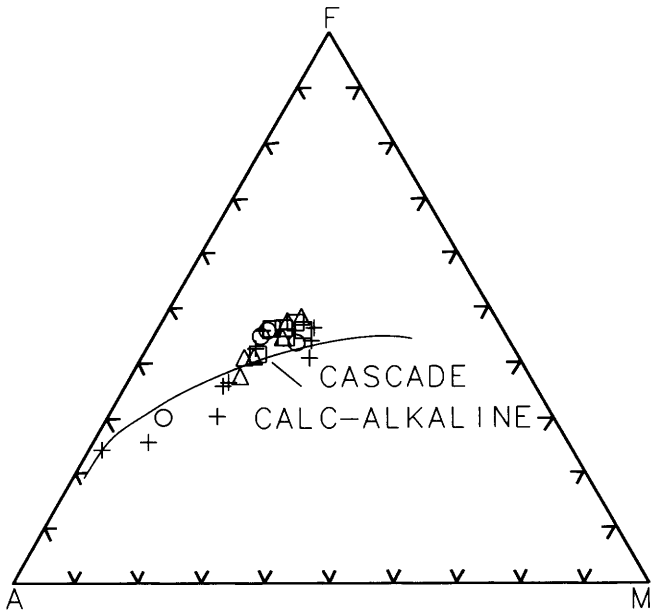

Figure 10. Ternary AFM diagram showing compositions of volcanic rock samples from the Sliderock Mountain stratovolcano. Cascade calc-alkaline trend line is from Irvine and Baragar (1971). See figure 6 for explanation of symbols.

compositional variation in the Sliderock Mountain stratovolcano rocks. The lack of a significant correlation between K_2O abundances and those of this group of oxides indicates that neither hornblende nor biotite were important in the geochemical evolution of these rocks.

Abundance variations of FeO and TiO_2 have an r^2 value of 0.73, and those of CaO and P_2O_5 have an r^2 value of 0.86. The lack of other oxide or element abundance covariations with these two pairs indicates that ilmenite and apatite, respectively, are additional phases that influenced compositional variation within the stratovolcano magmatic system. An additional consequence of fractional crystallization or varying degrees of partial melting is variable incompatible oxide or element enrichment of the resulting silicate liquid; a compositional covariation pair involving K_2O and Rb (r^2=0.84) may reflect either of these processes.

Hanson (1989) describes the use of trace element scatter plots in deciphering the petrogenesis of igneous rocks. Using plots of this type to model petrogenesis involves the use of the equations that define elemental abundances resulting from varying degrees of partial melting and (or) fractional crystallization. Following Shaw (1970), F is the fraction of liquid or melt in the system, D_i is the bulk distribution coefficient, C_{li} is the weight concentration of element I in the liquid or melt, and C_{oi} is the weight concentration of element I in the system. For melting, $C_{li}/C_{oi} = 1/[(1-F)D_i+F]$. If D_i is 0 for a given element (that is, if the element is completely incompatible), $C_{li}/C_{oi} = 1/F$ and the amount of melting can be constrained using an inferred C_{oi} and knowing the composition of samples that represent the system.

The equation for fractional crystallization (Neumann and others, 1954), $C_{li}/C_{oi} = F^{(Di-1)}$, also resolves to $C_{li}/C_{oi} = 1/F$ if D_i is 0, and the extent of fractional crystallization can be calculated.

An orthogonal plot in which the abundances of a highly incompatible element are plotted against those of a compatible element can be used to determine whether partial melting or fractional crystallization is principally responsible for the compositional evolution displayed by a suite of associated samples (Hanson, 1989). Rubidium, for instance, acts incompatibly in most igneous systems (Arth, 1976), especially in intermediate to mafic systems such as the one described here, whereas Sr behaves compatibly. The distribution of data for samples of the stratovolcano on a Rb-Sr plot (fig. 11) suggests that the liquid parental to these rocks contained about 40 ppm Rb and 1200 ppm Sr. Using that composition, assuming perfect Rb incompatibility (D_i=0), a bulk distribution coefficient of 2 (Arth, 1976) for Sr (in plagioclase and clinopyroxene), and the equations for melting and fractional crystallization, Rb and Sr abundances in liquids generated by varying amounts of melting or fractional crystallization can be calculated. Having done this, it is clear (fig. 11) that varying Rb and Sr abundances depicted by samples of the stratovolcano most probably result from fractional crystallization; compositions calculated for the relatively small amounts of melting necessary to produce the most evolved samples of the stratovolcano are characterized by Rb abundances that are far too large at any given Sr abundance. The curve calculated for varying degrees of fractional crystallization, however, fits the observed data fairly well. Deviations from the calculated fractional crystallization curve probably reflect analytical uncertainty and the weakly altered nature of Sliderock Mountain stratovolcano rocks.

Presuming that fractional crystallization is the dominant process responsible for compositional variation within samples of the stratovolcano, the fractional crystallization equation and abundance ranges of incompatible components, Rb for instance, can be used to evaluate the extent of crystallization required to produce the entire compositional abundance range. Because Rb abundances more than double, its D_i must be less than one (Hanson, 1989; fig. 1). For extents of fractional crystallization less than 0.8, D_i must be less than 0.3, which further indicates Rb incompatibility during evolution of the stratovolcano magmatic system. Finally, the incompatibility of Rb, as well as K_2O, is confirmed by a scatter plot for these components (fig. 12). Their incompatibility is indicated by colinearity of abundance variations and by the nearly zero y-intercept for the regression line through data for the stratovolcano. Using the regression line (instead of analytic data for individual samples, which may reflect weak rock alteration) the highest and lowest Rb contents in samples of the stratovolcano are about 105 and 40 ppm, respectively. So, 40/105=1/F and F=0.38; the extent of fractional crystallization (1-F) is 0.62. The most evolved sample of the Sliderock Mountain stratovolcano can be produced by 62 percent crystallization of a liquid represented by the most primitive sample.

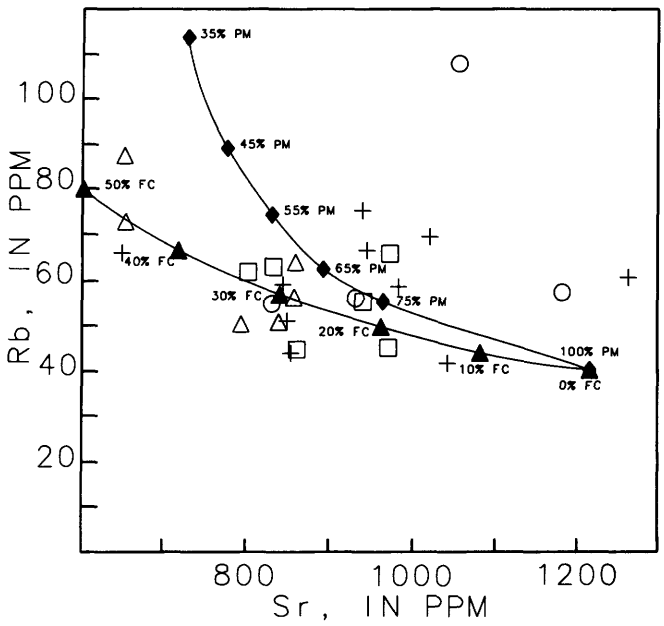

Figure 11. Variation diagram showing rubidium and strontium abundances in samples from the Sliderock Mountain stratovolcano (table 2). See figure 6 for explanation of symbols. Diamonds labeled 35% PM, 45% PM, 55% PM, 65% PM, 75% PM, and 100% PM are liquid compositions calculated for the indicated percentages of partial melting, as described in text; triangles labeled 50% FC, 40% FC, 30% FC, 20% FC, 10% FC, and 0% FC are liquid compositions calculated for the indicated percentages of fractional crystallization, as described in text.

REGIONAL TECTONO-MAGMATIC SPECULATION

Geochemical data presented here suggest that igneous products of the Sliderock Mountain stratovolcano are the products of arc-related magmatism. However, the Late Cretaceous age and position of the volcanic rocks of this field well east of the conventionally accepted locus (centered on the Idaho batholith) of Late Cretaceous arc magmatism is problematic. Dispersed magmatism, not coalesced to a narrow magmatic arc, and extending considerably inboard from inferred subduction zones has been presented (Lipman, 1980) as indicators of relatively low-angle subduction. The age and position of the Sliderock Mountain stratovolcano may indicate accelerated convergence and low-angle subduction along the Late Cretaceous western margin of North America.

Following development of the stratovolcano, Cenozoic magmatic activity, as represented by the Absaroka (Smedes and Prostka, 1972; Harlan and others, 1996) and Challis volcanic fields (Norman and others, 1992; Janecke and Snee,

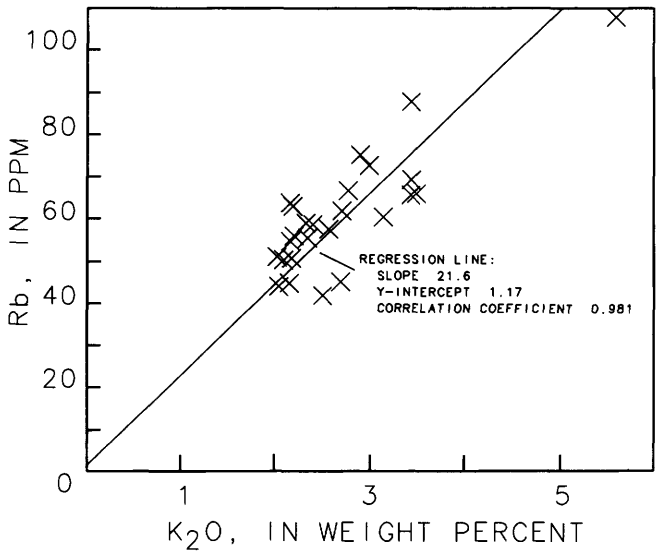

Figure 12. Variation diagram showing rubidium and potassium abundances in samples from the Sliderock Mountain stratovolcano (table 2).

1993), by renewed plutonism in south-central Idaho (Toth, 1987; Lewis and Kiilsgaard, 1991), and by alkalic magmatism in central Montana (Dudas, 1991) migrated westward across western Montana and into Idaho. Migration of the magmatic locus may represent decreased convergence and steeper subduction (Lipman, 1980) along the early Cenozoic western margin of North America as the subducted slab of oceanic lithosphere began to founder and the convecting asthenospheric wedge thickened (Lipman, 1980) in progressively westward positions beneath the western edge of the North American plate.

Dickinson and Hatherton (1967) demonstrated a relationship between the K_2O content (at a given SiO_2 content) of magma in subduction-related volcanic arc systems and depth to the center of the subducted slab (Benioff zone) beneath the arc. Lipman and others (1972) used this relationship and contoured the results to construct a map that portrays inferred depths to the Benioff zone beneath middle Cenozoic volcanic centers of the western United States. Their map (Lipman and others, 1972; fig. 9) indicates a depth of >310 km to the Benioff zone in the Sliderock Mountain area during middle Cenozoic time. The K_2O_{60} value of about 2.7 weight percent for the Late Cretaceous Sliderock Mountain stratovolcano (fig. 7) indicates a depth to the Benioff zone of about 225 km at 78–75 Ma. These observations imply that the convergence rate declined along the west edge of western North America and the angle of subduction steepened between Late Cretaceous and middle Cenozoic time in southern Montana. This suggestion is in accord with the westward retreat of arc magmatism represented by the Eocene Absaroka and Challis volcanic fields and the Eocene part of the Idaho batholith.

Finally, major crustal fault zones such as the Nye-Bowler lineament may have played a role in localizing volcanism along the southern margin of the Crazy Mountains Basin. The Nye-Bowler fault zone is a major northwest-trending zone of northeast- and northwest-trending wrench faults and folds caused by left-lateral fault movement during Late Cretaceous–early Tertiary time (Wilson, 1936; Roberts, 1972). The trend of the Nye-Bowler lineament is subparallel to that of the Lake Basin fault zone exposed to the north in the Crazy Mountains Basin and to a regionally extensive set of northwest-trending faults exposed throughout southwestern Montana (Schmidt and Garihan, 1986). Many of these faults, including those of the Nye-Bowler lineament, are thought to have originally formed during Precambrian extension, perhaps as normal faults associated with development of the Middle Proterozoic Belt Basin to the north and west. Many of the Proterozoic faults of southwestern and central Montana were reactivated as reverse and thrust faults during Late Cretaceous–early Tertiary contractional deformation to form major uplifts during the Laramide orogeny (Schmidt and Garihan, 1986). Some of these faults apparently localized intrusive and volcanic centers elsewhere in southwestern Montana. For example, Schmidt and others (1990) suggested that emplacement of the Late Cretaceous Tobacco Root batholith was controlled, at least in part, by northwest-trending left-oblique slip reverse faults that were active during Laramide contraction. Similarly, Chadwick (1970) suggested that two deep-seated northwest-trending faults, believed to be reactivated Precambrian fault zones, in the Beartooth Mountains, south of the study area, are responsible for the alignment of two chemically distinct, northwest-trending belts of Tertiary intrusions and volcanic centers of the Absaroka-Gallatin volcanic field. The northwest alignment of the Upper Cretaceous volcanic rocks and intrusions in the southern Crazy Mountains Basin, essentially astride the axis of the Nye-Bowler lineament, strongly suggests that this fault zone controlled the emplacement of volcanic centers of the field. The presence of deep-seated fault zones, as well as low-angle subduction along the western margin of North America at this time, may help explain the location of the Sliderock Mountain volcano field well east of the generally accepted locus of Late Cretaceous Cordilleran magmatism.

ACKNOWLEDGMENTS

Thanks to J.E. Elliott, B.S. Van Gosen, E.J. LaRock, and A.W. West who helped map the geology of the Sliderock Mountain area. Jane Hammarstrom provided the two sericite samples dated in this study and Ross Yeoman helped with the $^{40}Ar/^{39}Ar$ analyses. We thank local landowners for providing access across their land to public lands administered by the U.S. Forest Service. Technical reviews by Karen Lund and Ian Ridley helped improve this study.

REFERENCES

Arth, J.G., 1976, Behavior of trace elements during magmatic processes–A summary of theoretical models and their applications: U.S. Geological Survey Journal of Research, v. 4, p. 41–47.

Brozdowski, R.A., 1983, Geologic setting and xenoliths of the Lodgepole intrusive area—Implications for the northern extent of the Stillwater Complex, Montana: Philadelphia, Pa., Temple University, unpublished Ph.D. thesis, 322 p.

Chadwick, R.A., 1970, Belts of eruptive centers in the Absaroka-Gallatin volcanic province, Wyoming and Montana: Geological Society of America Bulletin, v. 81, p. 267–274.

Chappell, B.W., and White, A.J.R., 1992, I- and S-type granites in the Lachlan Fold Belt, *in* Brown, P.E., and Chappell, B.W., eds., Second Hutton symposium, the origin of granites and related rocks: Transactions of the Royal Society of Edinburgh, v. 83, p. 1–26.

Dalrymple, G.B., and Lanphere, M.A., 1969, Potassium-argon dating: San Francisco, W.H. Freeman Co., 251 p.

Dickinson, W.R., and Hatherton, T. 1967, Andesitic volcanism and seismicity around the Pacific: Science, v. 157, p. 801–803.

Dickinson, W.R., Klute, M.A., Hayes, M.J., Janecke, S.U., Lundin, E.R., McKittrick, M.A., and Olivares, M.D., 1988, Paleogeographic and paleotectonic setting of Laramide sedimentary basins in the central Rocky Mountain region: Geological Society of America Bulletin, v. 100, p. 1023–1039.

du Bray, E.A., 1995, Geochemistry and petrology of Oligocene and Miocene ash-flow tuffs of the southeastern Great Basin: U.S. Geological Survey Professional Paper 1559, 38 p.

du Bray, E.A., Elliott, J.E., Van Gosen, B.S., LaRock, E.J., and West, A.W., 1994, Reconnaissance geologic map of the Sliderock Mountain area, Sweet Grass County, Montana: U.S. Geological Survey Miscellaneous Field Studies Map MF–2259, scale 1:50,000.

du Bray, E.A., Ludington, Steve, Brooks, W.E., Gamble, B.M., Ratte, J.C., Richter, D.R., and Soria-Escalante, Eduardo, 1995, Compositional characteristics of middle to upper Tertiary volcanic rocks of the Bolivian Altiplano: U.S. Geological Survey Bulletin 2119, 30 p.

Dudas, F.O., 1991, Geochemistry of igneous rocks from the Crazy Mountains, Montana, and tectonic models for the Montana alkalic province: Journal of Geophysical Research, v. 96, p. 13261–13277.

Elsass, F., and du Bray, E.A., 1982, Energy-dispersive X-ray fluorescence spectrometry with the Kevex 7000 system: Saudi Arabian Deputy Ministry Mineral Resources Open File Report USGS-OF-02-52, 53 p.

Ewart, A., 1982, The mineralogy and petrology of Tertiary-Recent orogenic volcanic rocks with special reference to the andesitic-basaltic compositional range, *in* Thorpe, R.S., ed., Andesites: Chichester, Wiley, p. 25–87.

Fleck, R.J., Sutter, J.F., and Elliott, D.H., 1977, Interpretation of discordant $^{40}Ar/^{39}Ar$ age spectra of Mesozoic tholeiites from Antarctica: Geochimica et Cosmochimica Acta, v. 41, p. 15–32.

Fleck, R.J., Turrin, B.D., Sawyer, D.A., Warren, R.G., Champion, D.E., Hudson, M.R., and Minor, S.A., 1996, Age and character of basaltic rocks of the Yucca Mountain region, southern Nevada: Journal of Geophysical Research, v. 101, p. 8205–8227.

Gill, James, 1981, Orogenic andesites and plate tectonics: New York, Springer-Verlag, 390 p.

Hammarstrom, J.M., Zientek, M.L., and Elliott, J.E., 1993, Mineral resource assessment of the Absaroka-Beartooth study area, Custer and Gallatin National Forests, Montana: U.S. Geological Survey Open-File Report 93-207.

Hanna, W. F., 1973, Paleomagnetism of the late Cretaceous Boulder batholith, Montana: American Journal of Science, v. 273, p. 778–802.

Hanson, G.N., 1978, The application of trace elements to the petrogenesis of igneous rocks of granitic composition: Earth and Planetary Science Letters, v. 38, p. 26–43.

——— 1989, An approach to trace element modeling using a simple igneous system as an example, *in* Lipin, B.R., and McKay, G.A., eds. Geochemistry and mineralogy of rare earth elements: Reviews in Mineralogy, v. 21, p. 79–97.

Harlan, S.S., Geissman, J.M., Lageson, D.R., and Snee, L.W., 1988, Paleomagnetic and isotopic dating of thrust-belt deformation along the eastern edge of the Helena salient, northern Crazy Mountains Basin, Montana: Geological Society of America Bulletin, v. 100, p. 492–499.

Harlan, S.S., Snee, L.W., and Geissman, J.W., 1996, $^{40}Ar/^{39}Ar$ geochronology and paleomagnetism of Independence volcano, Absaroka Volcanic Supergroup, Beartooth Mountains, Montana: Canadian Journal of Earth Sciences, v. 33, p. 1648–1654.

Irvine, T.N., and Baragar, W.R.A., 1971, A guide to the chemical classification of volcanic rocks: Canadian Journal of Earth Sciences, v. 8, p. 523–548.

Janecke, S.U., and Snee, L.W., 1993, Timing and episodicity of middle Eocene volcanism and the onset of conglomerate deposition, Idaho: Journal of Geology, v. 101, p. 603–621.

Klepper, M.R., Ruppel, E.T., Freeman, V.L., and Weeks, R.A., 1971, Geology and mineral deposits, east flank of the Elkhorn Mountains, Broadwater County, Montana: U.S. Geological Survey Professional Paper 665, 66 p.

Lanphere, M.A., and Dalrymple, G.B., 1976, Identification of excess ^{40}Ar by the $^{40}Ar/^{39}Ar$ age spectrum technique: Earth and Planetary Science Letters, v. 32, p. 141–148.

Le Bas, M.J., Le Maitre, R.W., Streckeisen, A., and Zannetin, B., 1986, A chemical classification of volcanic rocks based on the total alkali-silica diagram: Journal of Petrology, v. 27, p. 745–750.

Lewis, R.S., and Kiilsgaard, T.H., 1991, Eocene plutonic rocks in south central Idaho: Journal of Geophysical Research, v. 96, p. 13295–13312.

Lipman, P.W., 1980, Cenozoic volcanism in the western United States–Implications for continental tectonics *in* Studies in Geophysics, Continental Tectonics: National Academy of Science, Washington, D.C., p. 161–174.

Lipman, P.W., Prostka, H.J., and Christiansen, R.L., 1972, Cenozoic volcanism and plate-tectonic evolution of the western United States—I. Early and middle Cenozoic: Philosophical Transactions of the Royal Society of London, Series A, v. 271, p. 217–248.

Ludwig, K.R., 1988, ISOPLOT Version 2—A plotting and regression program for isotope geochemists, for use with HP series 200/300 computers: U.S. Geological Survey Open-File Report 88-601, 49 p.

Macdonald, R., Smith, R.L., and Thomas, J.E., 1992, Chemistry of the subalkalic obsidians: U.S. Geological Survey Professional Paper 1523, 214 p.

Marvin, R.F., and Dobson, S.W., 1979, Radiometric ages—Compilation B, U.S. Geological Survey: Isochron/West, no. 26, p. 3–32.

Marvin, R.F., Mehnert, H.H., Naeser, C.W., and Zartman, R.E., 1989, U.S. Geological Survey radiometric ages—Compilation C part five—Colorado, Montana, Utah, and Wyoming: Isochron/West, no. 53, p. 14–19.

McDougall, I., and Harrison, T.M., 1988, Geochronology and thermochronology by the $^{40}Ar/^{39}Ar$ method: New York, Oxford University Press, 212 p.

Neumann, H., Mead, J., and Vitaliano, C.J., 1954, Trace element variation during fractional crystallization as calculated from the distribution law: Geochimica et Cosmochimica Acta, v. 6, p. 90–99.

Norman, M.D., Leeman, W.P., and Mertzman, S.A., 1992, Granites and rhyolites from the northwestern U.S.A.—Temporal variation in magmatic processes and relations to tectonic setting: Transactions of the Royal Society of Edinburgh, Earth Sciences, v. 83, p. 71–81.

Parsons, W.H., 1942, Origin and structure of the Livingston igneous rocks, Montana: Geological Society of America Bulletin, v. 53, p. 1175–1186.

Pearce, J.A., Harris, N.B.W., and Tindle, A.G., 1984, Trace element discrimination diagrams for the tectonic interpretation of granitic rocks: Journal of Petrology, v. 25, p. 956–983.

Roberts, A.E., 1972, Cretaceous and early Tertiary depositional history of the Livingston area, southwestern Montana: U.S. Geological Survey Professional Paper 526–C, 120 p.

Robinson, G.D., Klepper, M.R., and Obradovich, J.D., 1968, Overlapping plutonism, volcanism, and tectonism in the Boulder batholith region, western Montana, *in* Coats, R.R., Hay, R.L., and Anderson, C.A., eds., Studies in volcanology: Geological Society of America Memoir 116, p. 557–576.

Robinson, G.D., and Marvin, R.F., 1967, Upper Cretaceous volcanic glass from western Montana: Geological Society of America Bulletin, v. 78, p. 601–608.

Rouse, J.T., Hess, H.H., Foote, F., Vhay, J.S., and Wilson, K.P., 1937, Petrology, structure, and relation to tectonics of porphyry intrusions in the Beartooth Mountains, Montana: Journal of Geology, v. 45, p. 717–740.

Samson, S.D., and Alexander, E.C., Jr., 1987, Calibration of the interlaboratory $^{40}Ar/^{39}Ar$ dating standard, MMhb-1: Chemical Geology, v. 66, p. 27–34.

Schmidt, C.J., and Garihan, J.M., 1986, Role of recurrent movement of northwest-trending basement faults in the tectonic evolution of southwestern Montana: Proceedings of the 6th International Conference on Basement Tectonics, p. 1–15.

Schmidt, C.J., Smedes, H.W., and O'Neill, J.M., 1990, Syncompressional emplacement of the Boulder and Tobacco Root batholiths (Montana-U.S.A.) by pull-apart along old fault zones: Geological Journal, v. 25, p. 305–318.

Shaw, D.M., 1970, Trace element fractionation during anatexis: Geochimica et Cosmochimica Acta, v. 34, p. 237–243.

Smedes, H.W., 1966, Geology and igneous petrology of the northern Elkhorn Mountains, Jefferson and Broadwater Counties, Montana: U.S. Geological Survey Professional Paper 510, 116 p.

Smedes, W.H., and Prostka, H.J., 1972, Stratigraphic framework of the Absaroka Volcanic Supergroup in Yellowstone National Park: U.S. Geological Survey Professional Paper 729–C, 33 p.

Steiger, R.H., and Jäger, E., 1977, Subcommission on geochronology—Convention on the use of decay constants in geo- and cosmochronology: Earth and Planetary Science Letters, v. 36, p. 359–362.

Taggart, J.E., Lindsay, J.R., Scott, B.A., Vivit, D.V., Bartel, A.J., and Stewart, K.C., 1987, Analysis of geologic materials by X-ray fluorescence spectrometry, Chapter E *in* Baedecker, P.A., ed., Methods for geochemical analysis: U.S. Geological Survey Bulletin 1770, p. E1–E19.

Taylor, J.R., 1982, An introduction to error analysis: Mill Valley, Calif., University Science books, 270 p.

Tilling, R.I., 1973, Boulder batholith, Montana—A product of two contemporaneous but chemically distinct magma series: Geological Society of America Bulletin, v. 84, p. 3879–3900.

Tilling, R.I., Klepper, M.R., and Obradovich, J.D., 1968, K-Ar ages and time span of emplacement of the Boulder batholith, Montana: American Journal of Science, v. 266, p. 671–689.

Toth, M.I., 1987, Petrology and origin of the Idaho batholith, *in* Vallier, T.L., and Brooks, H.C., eds., Geology of the Blue Mountains region of Idaho, Oregon, and Washington: The Idaho Batholith and its border zone: U.S. Geological Survey Professional Paper 1436, p. 9–35.

Tysdal, R.G., Zimmerman, R.A., Wallace, A.R., and Snee, L.W., 1990, Geologic and fission-track evidence for Late Cretaceous faulting and mineralization, northeastern flank of Blacktail Mountains, southwestern Montana: U.S. Geological Survey Bulletin 1922, 20 p.

Vhay, J.S., 1934, The geology of a part of the Beartooth Mountain front near Nye, Montana: Princeton, N.J., Princeton University, unpublished Ph.D. thesis, 122 p.

Weed, W.H., 1893, The Laramie and the overlying Livingston Formation in Montana: U.S. Geological Survey Bulletin 105, 68 p.

Wilson, C.W., Jr., 1936, Geology of the Nye-Bowler lineament, Stillwater and Carbon Counties, Montana: American Association of Petroleum Geologists Bulletin, v. 20, p. 1161–1188.

Yager, D.B., and Quick, J.E., 1992, Superxap manual: U.S. Geological Survey Open-File Report 92-13, 45 p.

Manuscript approved for publication March 12, 1998
Published in the Central Region, Denver, Colorado
Graphics by the authors
Photocomposition by L.M. Carter and Joan G. Nadeau

☆ U.S. GOVERNMENT PRINTING OFFICE: 1998—673-048 / 20114 Region No. 8

Selected Series of U.S. Geological Survey Publications

Books and Other Publications

Professional Papers report scientific data and interpretations of lasting scientific interest that cover all facets of USGS investigations and research.

Bulletins contain significant data and interpretations that are of lasting scientific interest but are generally more limited in scope or geographic coverage than Professional Papers.

Water-Supply Papers are comprehensive reports that present significant interpretive results of hydrologic investigations of wide interest to professional geologists, hydrologists, and engineers. The series covers investigations in all phases of hydrology, including hydrogeology, availability of water, quality of water, and use of water.

Circulars are reports of programmatic or scientific information of an ephemeral nature; many present important scientific information of wide popular interest. Circulars are distributed at no cost to the public.

Fact Sheets communicate a wide variety of timely information on USGS programs, projects, and research. They commonly address issues of public interest. Fact Sheets generally are two or four pages long and are distributed at no cost to the public.

Reports in the **Digital Data Series (DDS)** distribute large amounts of data through digital media, including compact disc-read-only memory (CD-ROM). They are high-quality, interpretive publications designed as self-contained packages for viewing and interpreting data and typically contain data sets, software to view the data, and explanatory text.

Water-Resources Investigations Reports are papers of an interpretive nature made available to the public outside the formal USGS publications series. Copies are produced on request (unlike formal USGS publications) and are also available for public inspection at depositories indicated in USGS catalogs.

Open-File Reports can consist of basic data, preliminary reports, and a wide range of scientific documents on USGS investigations. Open-File Reports are designed for fast release and are available for public consultation at depositories.

Maps

Geologic Quadrangle Maps (GQ's) are multicolor geologic maps on topographic bases in 7.5- or 15-minute quadrangle formats (scales mainly 1:24,000 or 1:62,500) showing bedrock, surficial, or engineering geology. Maps generally include brief texts; some maps include structure and columnar sections only.

Geophysical Investigations Maps (GP's) are on topographic or planimetric bases at various scales. They show results of geophysical investigations using gravity, magnetic, seismic, or radioactivity surveys, which provide data on subsurface structures that are of economic or geologic significance.

Miscellaneous Investigations Series Maps or **Geologic Investigations Series (I's)** are on planimetric or topographic bases at various scales; they present a wide variety of format and subject matter. The series also incudes 7.5-minute quadrangle photogeologic maps on planimetric bases and planetary maps.

Information Periodicals

Metal Industry Indicators (MII's) is a free monthly newsletter that analyzes and forecasts the economic health of five metal industries with composite leading and coincident indexes: primary metals, steel, copper, primary and secondary aluminum, and aluminum mill products.

Mineral Industry Surveys (MIS's) are free periodic statistical and economic reports designed to provide timely statistical data on production, distribution, stocks, and consumption of significant mineral commodities. The surveys are issued monthly, quarterly, annually, or at other regular intervals, depending on the need for current data. The MIS's are published by commodity as well as by State. A series of international MIS's is also available.

Published on an annual basis, **Mineral Commodity Summaries** is the earliest Government publication to furnish estimates covering nonfuel mineral industry data. Data sheets contain information on the domestic industry structure, Government programs, tariffs, and 5-year salient statistics for more than 90 individual minerals and materials.

The Minerals Yearbook discusses the performance of the worldwide minerals and materials industry during a calendar year, and it provides background information to assist in interpreting that performance. The Minerals Yearbook consists of three volumes. Volume I, Metals and Minerals, contains chapters about virtually all metallic and industrial mineral commodities important to the U.S. economy. Volume II, Area Reports: Domestic, contains a chapter on the minerals industry of each of the 50 States and Puerto Rico and the Administered Islands. Volume III, Area Reports: International, is published as four separate reports. These reports collectively contain the latest available mineral data on more than 190 foreign countries and discuss the importance of minerals to the economies of these nations and the United States.

Permanent Catalogs

"Publications of the U.S. Geological Survey, 1879–1961" and **"Publications of the U.S. Geological Survey, 1962–1970"** are available in paperback book form and as a set of microfiche.

"Publications of the U.S. Geological Survey, 1971–1981" is available in paperback book form (two volumes, publications listing and index) and as a set of microfiche.

Annual supplements for 1982, 1983, 1984, 1985, 1986, and subsequent years are available in paperback book form.